
Rule-Bottleneck Reinforcement Learning: Joint Explanation and Decision Optimization for Resource Allocation with Language Agents

Mauricio Tec^{*12} Guojun Xiong^{*1} Haichuan Wang¹ Francesca Dominici² Milind Tambe¹³

Abstract

Deep Reinforcement Learning (RL) is remarkably effective in addressing sequential resource allocation problems in domains such as healthcare, public policy, and resource management. However, deep RL policies often lack transparency and adaptability, challenging their deployment alongside human decision-makers. In contrast, Language Agents, powered by large language models (LLMs), provide human-understandable reasoning but may struggle with effective decision making. To bridge this gap, we propose Rule-Bottleneck Reinforcement Learning (RBRL), a novel framework that jointly optimizes decision and explanations. At each step, RBRL generates candidate rules with an LLM, selects among them using an attention-based RL policy, and determines the environment action with an explanation via chain-of-thought reasoning. The RL rule selection is optimized using the environment rewards and an explainability metric judged by the LLM. Evaluations in real-world scenarios highlight RBRL’s competitive performance with deep RL and efficiency gains over LLM fine-tuning. A survey further confirms the enhanced quality of its explanations.

1. Introduction

Sequential resource allocation is a fundamental problem in many domains, including healthcare, finance, and public policy (Considine et al., 2025; Boehmer et al., 2024; Yu et al., 2024). This task involves allocating limited resources over time while accounting for dynamic changes and competing demands. Deep reinforcement learning (RL) is an effective

method to optimize decision-making for such challenges, offering efficient and scalable policies (Yu et al., 2021; Talaat, 2022; Xiong et al., 2023; Zhao et al., 2024). However, deep RL policies generally provide action recommendations without human-readable reasoning and explanations. Such lack of interpretability poses a major challenge in critical domains where decisions must be transparent, justifiable, and in line with human decision-makers to ensure trust and compliance with ethical and regulatory standards.

For example, doctors may need to decide whether to prioritize intervention for Patient A or Patient B based on their current vital signs (Boehmer et al., 2024). An RL algorithm might suggest: “*Intervene with Patient A*” with the implicit goal of maximizing the value function. However, the underlying reasoning may not be clear to the doctors, leaving them uncertain about the factors influencing the decision (Milani et al., 2024). For doctors, a more effective suggestion could be risk-based with specific information, e.g., “*Patient A’s vital signs are likely to deteriorate leading to higher potential risk compared to Patient B, so intervention with Patient A is prioritized*” (Gebrael et al., 2023; Boatin et al., 2021).

Language agents (Sumers et al., 2024) leverage large language models (LLMs) for multi-step decision-making using reasoning techniques like chain of thought (CoT) (Wei et al., 2022) and ReAct (Yao et al., 2023). They enable natural language goal specification (Du et al., 2023) and enhance human understanding (Hu & Sadigh, 2023; Srivastava et al., 2024). However, LLMs struggle with complex sequential decision-making, such as resource allocation (Furuta et al., 2024), making RL a crucial tool for refining them into effective policy networks (Carta et al., 2023; Tan et al., 2024; Wen et al., 2024; Zhai et al., 2024). Yet, fine-tuning LLMs for policy learning is highly challenging due to the substantial computational costs and the complexity of token-level optimization (Rashid et al., 2024), which remains an open challenge, particularly in sequential resource allocation.

Consequently, aiming to combine the strengths of both deep RL and language agents, we pose the following question:

^{*}Equal contribution ¹Department of Computer Science, Harvard John A. Paulson School of Engineering and Applied Sciences ²Department of Biostatistics, Harvard T.H. Chan School of Public Health ³Google DeepMind. Correspondence to: Mauricio Tec <mauriciogtec@g.harvard.edu>, Guojun Xiong <gjxiong@g.harvard.edu>.

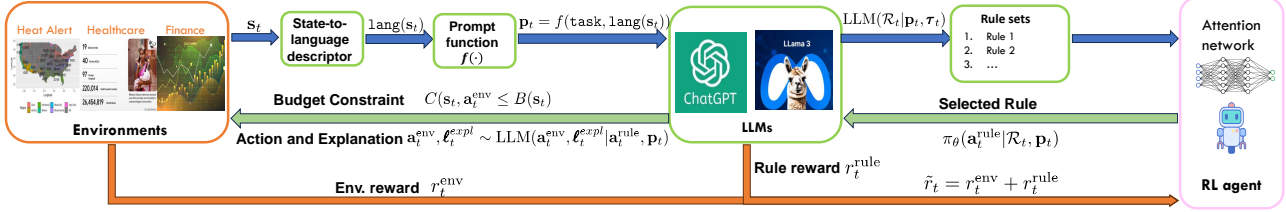


Figure 1: Overview of the RBRL framework for joint sequential decision-making and explanation generation at time instance t . Starting with current state s_t , a state-to-language descriptor generates $\text{lang}(s_t)$, which is used to create the input prompt \mathbf{p}_t . The LLM processes \mathbf{p}_t to produce a thought τ_t and a set of candidate rules \mathcal{R}_t . An attention-based policy network selects a rule $\mathbf{a}_t^{\text{rule}}$, which is used to derive an executable action $\mathbf{a}_t^{\text{env}}$ satisfying the budget constraint $B(s_t)$ for the environment and a human-readable explanation ℓ_t^{expl} , while also providing a rule reward r_t^{rule} . The environment transitions to the next state s_{t+1} , returning an environment reward r_t^{env} . This process is repeated iteratively at subsequent time steps.

Can we design a language agent framework that can simultaneously perform sequential resource allocation and provide human-readable explanations?

Motivated by existing work that employs predefined rules or concepts to explain RL policies (Das et al., 2023) or guide RL exploration (Likmeta et al., 2020), we explore the potential of using rules to prioritize individuals in resource allocation problems. In the context of language agents, rules are defined as “structured statements” that capture prioritization among choices in a given state, aligning with the agent’s goals (Srivastava et al., 2024). Rules offer a flexible framework for encoding high-level decision criteria and priority logic, similar as the celebrated index policy for prioritizing arms in resource allocation problems (Whittle, 1988), making them ideal for guiding resource allocation strategies while explaining the rationale behind decisions.

Building on this, we propose a novel framework called Rule-Bottleneck Reinforcement Learning (RBRL), which integrates the strengths of LLMs and RL to bridge the gap between decision-making and interoperability, by optimizing LLM-generated rules with RL. RBRL provides a framework (as shown in Figure 1) that simultaneously makes sequential resource allocation decisions and provides human-readable explanations. RBRL leverages LLMs to generate candidate rules and employs RL to optimize policy selection, enabling the creation of effective decision policies while simultaneously providing human-understandable explanations.

Our contributions are summarized as follows. *First*, to avoid the computational cost and complexity of directly fine-tuning language agents, we leverage LLMs to generate a diverse set of rules, where each rule serves as a prioritization strategy for individuals in resource allocation. This approach enhances flexibility and interpretability in decision-making. *Second*, we extend the conventional state-action space by integrating the thoughts and rules generated by LLMs, creating a novel framework that enables reinforcement learning to operate on a richer, more interpretable

decision structure. *Third*, we introduce an attention-based training framework that maps states to queries and rules to keys. The rule selection process is optimized by a policy network trained using the Soft Actor-Critic (SAC) algorithm (Haarnoja et al., 2018), ensuring robust and efficient decision-making. In particular, the LLM also acts as a feedback mechanism, providing guidance during RL exploration to improve policy optimization and promote more effective learning.

We evaluate our method in three environments from two real-world domains: `HeatAlerts`, where resources are allocated to mitigate extreme heat events; and `WearableDeviceAssignment`, for distributing monitoring devices to patients. Using cost-effective LLMs such as gpt-4o-mini (OpenAI, 2024b) and Llama 3.1 8B (Meta AI, 2024), we first assess decision performance by comparing RBRL with pure RL methods and language agent baselines. We then evaluate explanation quality through a human survey conducted under IRB approval. The results demonstrate RBRL’s effectiveness in both decision quality and interpretability.

2. Related Work

Our work intersects with three distinct areas within the RL literature. We discuss related work in each of these domains.

RL for Resource Allocation RL has been widely studied for constrained resource allocation across domains. In maternal health, Boehmer et al. (2024) apply RL to a restless multiarmed bandit (RMAB) problem (Whittle, 1988) to compute patient-specific intervention probabilities. Also in an RMAB setting, Xiong et al. (2022) propose a model-based RL approach that prioritizes users via an index and allocates resources under budget constraints. In public health, Considine et al. (2025) propose RL to optimize extreme heat warnings under a budget on the number of possible alerts. Other works include multi-agent RL for robotic warehouse allocation (Shen et al., 2023) and exogenous

MDPs for cloud resource management (Sinclair et al., 2023). While these methods optimize rewards effectively, they often lack interpretability—critical for deployment in sensitive domains requiring trust, transparency, and accountability.

RL and Language Agents The language agents (Sumers et al., 2024) paradigm developed somewhat independently of RL, with works like ReAct prompting (Yao et al., 2023) extending chain-of-thought (CoT) (Wei et al., 2022) to action settings. These works have focused on tasks such as open-ended web navigation (Putta et al., 2024), social simulations (Park et al., 2023), and virtual assistants (Vezhnevets et al., 2023). Meanwhile, language interfaces have also been proposed within the RL literature, including leveraging external and commonsense knowledge (Feng et al., 2024; Waytowich et al., 2024), pre-training goal-based policies (Du et al., 2023), enhancing generalization in embodied agents (Szot et al., 2023), and aiding human-AI coordination (Srivastava et al., 2024; Hu & Sadigh, 2023). Related works include GLAM (Carta et al., 2023), TWOSOME (Tan et al., 2024), BAD (Wen et al., 2024), and TextGym (Xi et al., 2024), which use LLM finetuning techniques in RL environments with a reward function. Relevant to our work is also Wang et al. (2023), which, inspired by open-ended settings like Minecraft, employs RL to optimize the goals of an LLM planner based on feasibility.

Explainable RL (XRL) Early XRL relied on methods like decision trees and concept-based explanations (Das et al., 2023), but these struggled with scalability in dynamic environments (Poeta et al., 2023). Recent advances introduced large language models (LLMs) for post-hoc explanations, such as explaining decision paths from policy trees (Zhang et al., 2023) or adding language descriptions to RL policies (Colas et al., 2022). However, these approaches focus on interpreting pre-existing policies rather than enabling LLMs to generate inherently explainable decisions, with challenges in aligning explanations to human reasoning (Singh et al., 2024). By contrast, inherently (also known as intrinsically) interpretable policies are those that have internal representation that allow explanations (Peng et al., 2022; Milani et al., 2024). Our work sits this literature by using LLM reasoning traces as the basis for environment action selection.

With various works acknowledging the trade-off between interpretability and performance, prioritizing interpretability appears to be crucial in practice for many critical applications (Rudin, 2019): an approach that we subscribe to in this work. For example, in the clinical AI domain, physicians require transparency to validate recommendations and uphold ethical accountability, as mandated by regulatory frameworks (e.g., EPC (2024); CSL (2024)). High-performing black-box systems often face rejection in clinical workflows due to distrust (Shevtsova et al., 2024; DuBois, 2019). By

contrast, interpretable models allow clinicians to audit biases and adapt logic to local contexts, whereas opaque policies risk failures under real-world distribution shifts (Rudin, 2019; Doshi-Velez & Kim, 2017). Transparent reasoning facilitates iterative, clinician-driven refinement, ensuring collaborative decision aid rather than an inflexible oracle (Shevtsova et al., 2024; DuBois, 2019). Empirical surveys show clinicians favor models that enable shared decision-making, error accountability, and ethical oversight despite modest performance penalties (Shevtsova et al., 2024)—a critical stance in high-stakes healthcare environments where trust and adaptability outweigh narrow efficiency gains.

3. Preliminaries and Problem Formulation

Notations. A bold lowercase letter $\mathbf{a} \in \mathbb{R}^d$ represents a vector with dimension d , while a regular lowercase letter a denotes a scalar. An uppercase letter A denotes a mapping function, and a calligraphic letter \mathcal{A} denotes a set; $[h]$ denotes the set of $\{1, \dots, h\}$; $\Delta(\mathcal{A})$ denotes the space of probability distributions supported in \mathcal{A} .

3.1. Resource-Constrained Allocation

Resource-constrained allocation tasks are usually formulated as a special Constrained Markov Decision Process (CMDP), which is defined by the tuple $\langle \mathcal{S}, \mathcal{A}, P, R, C, h, \gamma \rangle$, where \mathcal{S} denotes a state space and \mathcal{A} denotes a finite action space. The transition probability function, specifying the probability of transitioning to state $s' \in \mathbb{R}^{d_1}$ after taking action $\mathbf{a} \in \mathbb{R}^{d_2}$ in state s , is $P(s'|s, \mathbf{a}) : \mathcal{S} \times \mathcal{A} \times \mathcal{S} \rightarrow \Delta(\mathcal{S})$, $R(s, \mathbf{a}) : \mathcal{S} \times \mathcal{A} \rightarrow \mathbb{R}$ represents the reward function, defining the immediate reward received after taking action \mathbf{a} in state s , and we let $C(s, \mathbf{a}) : \mathcal{S} \times \mathcal{A} \rightarrow \mathbb{R}^{d_3}$ be the immediate cost incurred after taking action \mathbf{a} in state s . Often, each dimension $i \in [d_2]$ in \mathbf{a} is either 0 or 1 in resource-constrained allocation tasks. In addition, h is the time horizon and $\gamma \in [0, 1]$ denotes the discount factor, which determines the present value of future rewards.

The goal of resource-constrained allocation tasks is to find a policy $\pi : \mathcal{S} \rightarrow \Delta(\mathcal{A})$ that maximizes the expected cumulative discounted reward while satisfying the cost constraints:

$$\pi^* = \arg \max_{\pi} \mathbb{E}_{\pi} J(\pi) := \left[\sum_{t=1}^h \gamma^{t-1} R(\mathbf{s}_t, \mathbf{a}_t) \right]$$

$$s.t. \quad \forall t \in [h]: C(\mathbf{s}_t, \mathbf{a}_t) \leq B(\mathbf{s}_t), \quad (1)$$

where $B : \mathcal{S} \rightarrow \mathbb{R}^{d_3}$ is the budget function.

3.2. Language-augmented RL with Rules

We outline the language-augmented RL framework, where the action space includes internal language actions $\tilde{\mathcal{A}} = \mathcal{A} \cup \mathcal{L}$ (Yao et al., 2023; Carta et al., 2023). Language

Example Language Wrapper for Heat Alert Issuance

Task: Assist policymakers in deciding when to issue public warnings to protect against heatwaves. Your goal is to minimize the long-term impact on health and mortality. Your decision should be based on the remaining budget, weather conditions, day of the week, past warning history, and remaining warnings for the season. The goal is to issue warnings when they are most effective, minimizing warning fatigue and optimizing for limited resources.

Action: A single integer value representing the decision: 1 = issue a warning, 0 = do not issue a warning. Warning can only be issued if the 'Remaining number of warnings/budget' is positive. Response in JSON format. For example: {'action': 1}.

(a) Examples of initial task prompt, which contains the task description and available actions.

Step 1: Generate Thoughts
<p>Two example thoughts:</p> <ul style="list-style-type: none"> - There are only four warnings remaining in the budget. - The current heat index is high, and issuing alert could raise public awareness.
Step 2: Generate Rules Based on Thoughts and the Current State
<p>An example rule:</p> <ul style="list-style-type: none"> - Background: Maintaining a balance in warning issuance is crucial for future effectiveness. - Rule: If there are 3 or more warnings remaining, issue a warning when the heat index is above 105 F. - State Relevance: There are 4 warnings remaining, allowing for proactive issuance given the current heat index of 107 F.

(b) Examples of generated rules for the Heat Alert Issuance task.

Figure 2: Examples of task prompts and generated rules.

agents typically have two types of internal language actions: First, *thoughts* $\mathbf{a}^{\text{thought}} \in \mathcal{L}$, are reasoning traces from the current problem state used to inform environment action selection $\mathbf{a}^{\text{env}} \in \mathcal{A}$ (Yao et al., 2023). Second, *post-hoc explanations* ℓ^{expl} , are generated from actions and thoughts to enhance human trust and interpretability (Zhang et al., 2023), a focus of this work.

Rules Thoughts are useful to highly relevant aspects of a problem. However, they often lack detailed information to identify the next optimal action. In this work, we will consider “rules” $\mathbf{a}^{\text{rule}} \in \mathcal{L}$, which are structured language statements derived from thoughts that generally take the form “[do/prioritize] [if/when]”. More formally, each rule \mathbf{a}^{rule} consists of a triple (background, rule_statement, state_relevance). Figure 2b shows examples of generated rules from one of the domains used in the experiments.

Task and Constraints Description Language agents require: (1) a language description of the environment and the agent’s goal, denoted task ; (2) a function describing the state of the environment in natural language, denoted $\text{lang} : \mathcal{S} \rightarrow \mathcal{L}$. At each state s_t , these descriptors are used to construct a natural language prompt $\mathbf{p}_t = f(\text{task}, \text{lang}(s_t), C, B)$, where C and B are the costs and budget constraints defined in eq. (1). For instance, the prompt can restrict certain actions, or the total number of allocations in a given period of time. Figure 2a exemplifies rules generated for the environments in our experiments.

Baseline Rule-based Language Policy Our objective is

to jointly optimize the reward and explainability of the environment. Hence, we will take as baseline an LLM-driven policy π_{LLM} for online interaction with the environment:

$$\mathbf{a}_t^{\text{thought}} \sim \pi_{\text{LLM}}(\mathbf{a}_t^{\text{thought}} \mid \mathbf{p}_t), \quad (2)$$

$$\mathbf{a}_t^{\text{rule}} \sim \pi_{\text{LLM}}(\mathbf{a}_t^{\text{rule}} \mid \mathbf{a}_t^{\text{thought}}, \mathbf{p}_t), \quad (3)$$

$$\mathbf{a}_t^{\text{env}} \sim \pi_{\text{LLM}}(\mathbf{a}_t^{\text{env}} \mid \mathbf{a}_t^{\text{rule}}, \mathbf{a}_t^{\text{thought}}, \mathbf{p}_t), \quad (4)$$

$$\ell_t^{\text{expl}} \sim \pi_{\text{LLM}}(\ell_t^{\text{expl}} \mid \mathbf{a}_t^{\text{env}}, \mathbf{a}_t^{\text{rule}}, \mathbf{p}_t). \quad (5)$$

The rule acts as a “bottleneck” to the action and explanation.

Remark 3.1. This baseline builds on the baseline chain-of-thought language agent, augmented by the generation of a single rule $\mathbf{a}_t^{\text{rule}}$. In the next section, we will introduce RBRL, which replaces the generation of a single $\mathbf{a}_t^{\text{rule}}$ with an RL-based learnable selection policy π_θ choosing among a set of dynamically generated candidate rules.

Explainability Explainability in AI encompasses multiple dimensions (see Hoffman et al. (2018) for an overview). Here, we evaluate the explainability of \mathbf{a}^{rule} and ℓ^{expl} through two key aspects:

1. *Completeness of \mathbf{a}^{rule} :* Can the optimal action be predicted from the rule? Does it contain sufficient detail about its applicability to the current state?
2. *Trust and understanding with ℓ^{expl} :* Do humans find the explanation useful to understand the system behavior? Does it foster trust in the system?

Analyzing both \mathbf{a}^{rule} and ℓ^{expl} is critical since post hoc LLM explanations alone may be prone to “satisfying” but misleading rationalizations (Zhang et al., 2023). We hypothesize that complete rules aid to generating better post-hoc explanations by outlining a more structured reasoning process.

3.3. Problem Statement

Our primary challenge is to enable LLMs to jointly optimize a language policy that both solves the underlying optimization problem and enhances the quality of the explanations—a task that has received little attention in the literature. We aim to increase the quality of ℓ^{expl} while also optimizing decision-making. We aim to achieve this by selecting rules that encourage both good quality explanations and high reward. In Section 4, we will describe our method for constructing a surrogate explainability “rule reward” $R_{\text{LLM}}^{\text{rule}}(\mathbf{a}^{\text{rule}})$ using an LLM as judge (Shen et al., 2024; Bhattacharjee et al., 2024; Gu et al., 2024). We denote the joint environment/rule reward as $\tilde{r}_t = R(s_t, \mathbf{a}_t^{\text{env}}) + R_{\text{LLM}}^{\text{rule}}(\mathbf{a}_t^{\text{rule}})$. Then, we propose the following augmented optimization objective:

$$\max_{\pi} \mathbb{E}_{\pi} \tilde{J}(\pi) := \left[\sum_{t=1}^h \gamma^{t-1} \tilde{r}_t \right] \text{ s.t. constraint in (1).} \quad (6)$$

We emphasize that LLMs cannot fully replace the ultimate human assessment, but they they provide a scalable alternative during the optimization process.

4. Rule-based Reinforcement Learning (RBRL)

RBRL leverages the strengths of LLMs and RL to achieve both interpretability and robust sequential decision-making.

Algorithm Overview The RBRL framework in ALgorithm 1 involves four steps: (1) RULE SET GENERATION (line 3), the LLM processes the state-task \mathbf{p}_t to create candidate rules \mathcal{R}_t for action selection; (2) RULE SELECTION (line 4), an attention-based RL policy π_θ selects the best rule $\mathbf{a}_t^{\text{rule}} \in \mathcal{R}$; (3) DECISION, RULE REWARD AND EXPLANATION (lines 5-8), the LLM generate an environment action $\mathbf{a}_t^{\text{env}}$ and based on the chosen rule $\mathbf{a}_t^{\text{rule}}$ and gives a human-readable explanation ℓ_t^{expl} ; (4) REINFORCEMENT LEARNING (lines 10-12), collected samples update the policy π_θ and value networks with the SAC algorithm (Haarnoja et al., 2018) and the combined environment and rule reward \tilde{r}_t . Algorithm 1 details the entire process. Further sections elaborate on these steps.

Algorithm 1 RBRL

Require: Rule-selection policy π_θ ; Value network $\{Q_\phi^j\}_{j \in \{1,2\}}$; and Replay buffer \mathcal{B} .

- 1: **Initialization:** Initial state \mathbf{s}_0 and task-state prompt \mathbf{p}_0 .
- 2: **for** $t = 0, \dots, \text{max_iters} - 1$ **do**
- 3: Generate rule candidates \mathcal{R}_t using CoT from \mathbf{p}_t and $\mathbf{a}_t^{\text{thought}}$. // Section 4.1
- 4: Select rule $\mathbf{a}_t^{\text{rule}}$ using the RL policy π_θ from \mathcal{R}_t and \mathbf{s}_t . // Section 4.2
- 5: Generate the environment action $\mathbf{a}_t^{\text{env}}$ with the LLM from $\mathbf{a}_t^{\text{rule}}$, \mathbf{p}_t , and previous thoughts.
- 6: Apply the action in the environment and obtain new state \mathbf{s}_{t+1} and environment reward $\mathbf{r}_t^{\text{env}}$.
- 7: Generate post-hoc explanation with the LLM from $\mathbf{a}_t^{\text{env}}$, $\mathbf{r}_t^{\text{rule}}$, \mathbf{p}_t , and previous thoughts.
- 8: Generate rule reward \mathbf{r}^{rule} with the LLM as judge. // Section 4.3
- 9: Update the prompt \mathbf{p}_{t+1} from \mathbf{s}_{t+1} , and the constraints \mathcal{C} and budget B .
- 10: Append transition to the replay buffer $\mathcal{B} \leftarrow \mathcal{B} \cup \{(\tilde{\mathbf{s}}_t, \mathbf{a}_t^{\text{rule}}, \tilde{r}_t, \tilde{\mathbf{s}}_{t+1})\}$ where $\tilde{\mathbf{s}}_t = (\mathbf{s}_t, \mathcal{R}_t)$ and $\tilde{r}_t = r_t^{\text{rule}} + r_t^{\text{env}}$.
- 11: **if** $t \bmod k = 0$ **then**
- 12: Sample from the replay buffer and use Soft-Actor Critic RL to update the policy network $\pi_\theta(\mathbf{a}_t^{\text{rule}}|\tilde{\mathbf{s}}_t)$ and value networks $\{Q_\phi^j(\tilde{\mathbf{s}}_t, \mathbf{a}_t^{\text{rule}})\}_{j \in \{1,2\}}$. // Section 4.4
- 13: **end if**
- 14: **end for**

4.1. Rule Set Generation

The rule generation process seeks to create interpretable and actionable guidelines for decision-making. Under this framework, a set of candidate rules \mathcal{R}_t is generated according to $\mathcal{R}_t \sim \pi_{\text{LLM}}(\mathcal{R}_t|\mathbf{p}_t, \mathbf{a}_t^{\text{thought}})$. To enhance interpretability, each rule is accompanied by a rationale explaining the reasoning behind the decision. The LLM is instructed to generate rules as a JSON format, which is common for integration of LLMs with downstream applications (Together AI, 2024). Examples of generated rules are given in Figure 2b. See Figure 10 in the Appendix for the prompt templates used to generate the rules.

A higher number of rules is always preferable, however, it also increases the generating costs and slows down each iteration of the method. For our experiments, we found that $|\mathcal{R}_t| = 5$ provided achieved a reasonable trade-off.

4.2. Rule Selection

In this step, rules are converted from text to vector form, and a trainable attention-based policy network π_θ provides the probability distribution for sampling a rule. Figure 3 illustrates the process, with a detailed procedure in Algorithm 2 of the Appendix. Below are the major components of the architecture of π_θ . We propose to base the architecture on cross-attention layers (Bahdanau et al., 2015; Vaswani et al., 2017), with the state acting as the keys and values, and the rules as the queries. This allows to learn from the embedding representations of rules, and efficiently handle dynamically changing number of rules if needed.

State Representation. The numeric state is projected by a linear layer: $\mathbf{k}_t = \text{Linear}(\mathbf{s}_t) \in \mathbb{R}^{d_h}$, with d_h being to denote the architecture hidden dimension.

Rule Candidate Embedding. Each rule in the list of rule candidates $\mathcal{R}_t = \{\rho_1^t, \rho_2^t, \dots, \rho_q^t\}$ is embedded into a numeric representation using a Sentence Embedding language model (e.g., SentenceBERT (Reimers & Gurevych, 2019)) and further processed by a projection layer similar to the state representation. This results in a *query* matrix $\mathbf{Q}_t \in \mathbb{R}^{q \times d_h}$.

Attention-based Policy Network. The vector \mathbf{k}_t , serving as keys, engages with the rule embeddings \mathbf{Q}_t , acting as queries, via a cross-attention mechanism to derive a hidden state representation $\mathbf{h}_t^{(1)} = \text{Attention}(\mathbf{Q}_t, \mathbf{k}_t^\top, \mathbf{k}_t^\top) \in \mathbb{R}^{q \times d_h}$, computed as

$$\text{Attention}(\mathbf{Q}_t, \mathbf{k}_t^\top, \mathbf{k}_t^\top) = \text{softmax}\left(\frac{\mathbf{Q}_t \mathbf{k}_t^\top}{\sqrt{d_h}}\right) \mathbf{k}_t^\top,$$

which facilitates the rule candidate vector embeddings in attending to the environment state. Subsequently, we sequentially apply self-attention layers to the hidden representation $\mathbf{h}^{(k+1)} = \text{Attention}(\mathbf{h}_t^{(k)}, \mathbf{h}_t^{(k)}, \mathbf{h}_t^{(k)})$, enabling

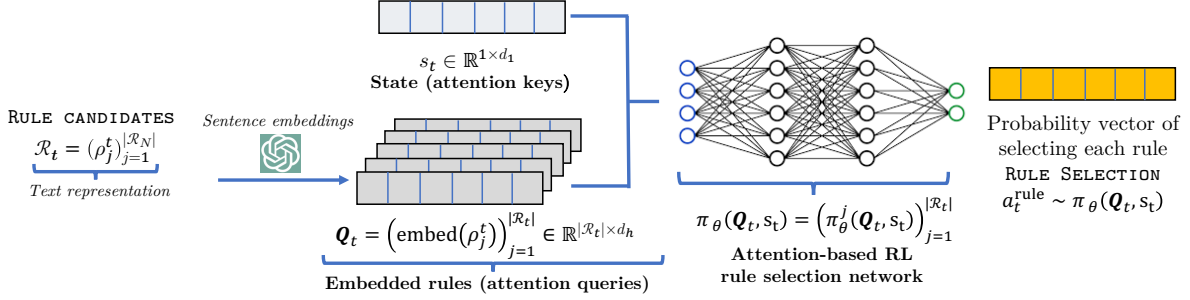


Figure 3: Overview of the RULE SELECTION step. The current state is encoded as a key vector, while candidate rules are encoded as Queries using a text embedding API (e.b., BERT sentence embedding). An attention-based policy network π_θ trained with SAC computes a probability distribution over the candidate rules, enabling the selection of the most suitable rule for decision-making and explanation.

the rule embeddings to attend to one another to rank an optimal candidate. Ultimately, following $K - 1$ self-attention layers, a final linear layer converts the rule representations into logit vectors $\alpha_\theta^t = \text{Linear}(\mathbf{h}_t^{(k)}) \in \mathbb{R}^q$ used for the computation of the probability of selecting each rule.

For the implementation, the attention layer is realized using the multi-headed attention module from Vaswani et al. (2017). We incorporate a dropout layer, fixed at 0.05 for the experiments, along with SiLU activation and layer normalization, which are excluded from the notation for brevity.

Rule Selection. The policy distribution over the rules:

$$\pi_{\theta,i}(\mathbf{Q}_t, \mathbf{k}_t) = \frac{\exp(\alpha_{\theta,i}^t(\mathbf{Q}_t, \mathbf{k}_t))}{\sum_{j=1}^q \exp(\alpha_{\theta,j}^t(\mathbf{Q}_t, \mathbf{k}_t))}, \quad i = 1, \dots, q.$$

A rule is selected sampled from the distribution: $\mathbf{a}_t^{\text{rule}} \sim \text{Categorical}(\mathcal{R}; (\pi_{\theta,i}(\mathbf{Q}_t, \mathbf{k}_t))_{i=1}^q)$.

4.3. Decision, Rule Reward, and Explanation

Upon selection of rule $\mathbf{a}_t^{\text{rule}}$, the LLM determines the action to be applied within the environment $\mathbf{a}_t^{\text{env}} \sim \pi_{\text{LLM}}(\mathbf{a}_t^{\text{env}} | \mathbf{a}_t^{\text{rule}}, \mathbf{a}_t^{\text{thought}}, \mathbf{p}_t)$, ensuring concordance with the chosen strategy. Subsequently, the LLM formulates a post-hoc explanation $\ell_t^{\text{expl}} \sim \pi_{\text{LLM}}(\ell_t^{\text{expl}} | \mathbf{a}_t^{\text{env}}, \mathbf{a}_t^{\text{rule}}, \mathbf{a}_t^{\text{thought}}, \mathbf{p}_t)$ contingent upon the rule. Figure 10 in the Appendix illustrates the prompt template employed to generate both the action and explanation.

This procedure concurrently produces the rule reward $R_{\text{LLM}}^{\text{rule}}(r_t^{\text{rule}})$, used for reinforcement learning (RL) in the next step. This reward is derived from using the LLM as a judge to answer the following three questions:

ER₁. Without providing $\mathbf{a}_t^{\text{env}}$, is $\mathbf{a}_t^{\text{rule}}$ sufficient to predict/infer the optimal action?

ER₂. Does $\mathbf{a}_t^{\text{rule}}$ contain enough details about the applicability of the rule to the current state?

ER₃. Given $\mathbf{a}_t^{\text{env}}$, is $\mathbf{a}_t^{\text{rule}}$ compatible with this selection?

Each question scores as 0 if negative or 1 if positive. The rule reward is calculated as $r_t^{\text{rule}} = R_{\text{LLM}}^{\text{rule}}(\mathbf{a}_t^{\text{rule}}) = (1/3) \sum_i \text{ER}_i$. Refer to Figure 10 in the Appendix for the full prompt.

4.4. RL with SAC

Augmented state space Traditional RL frameworks fail here due to intermediate steps: generating the rule set \mathcal{R}_t , mapping rules $\mathbf{a}_t^{\text{rule}}$ to actions $\mathbf{a}_t^{\text{env}}$ in an LLM-driven environment. RBRL addresses this issue by creating an augmented state $\tilde{\mathbf{s}}_t := (\mathbf{s}_t, \mathcal{R}_t)$ with transition dynamics $P(\tilde{\mathbf{s}}_{t+1} | \tilde{\mathbf{s}}_t, \mathbf{a}_t^{\text{rule}})$, integrating rules into the state space for reasoning over both the environment’s dynamics and decision rules $\mathbf{a}_t^{\text{rule}}$. This proposition explains the transition computation.

Theorem 4.1. *The state transition of the RBRL MDP can be calculated as*

$$P(\tilde{\mathbf{s}}_{t+1} | \tilde{\mathbf{s}}_t, \mathbf{a}_t^{\text{rule}}) = P(\mathcal{R}_{t+1} | \mathbf{s}_{t+1}) \times \int_{\mathbf{a}} P(\mathbf{s}_{t+1} | \mathbf{a}^{\text{env}}, \mathbf{s}_t) \cdot P(\mathbf{a}^{\text{env}} | \mathbf{a}_t^{\text{rule}}, \mathbf{s}_t) d\mathbf{a}^{\text{env}}, \quad (7)$$

where $P(\mathcal{R}_{t+1} | \mathbf{s}_{t+1}) = \pi_{\text{LLM}}(\mathcal{R}_{t+1} | \mathbf{p}_t, \boldsymbol{\tau}_t)$ is the probability of the LLM generating rule set \mathcal{R}_{t+1} provided the state \mathbf{s}_{t+1} , $P(\mathbf{s}_{t+1} | \mathbf{a}^{\text{env}}, \mathbf{s}_t)$ is the original environment dynamics, and $P(\mathbf{a}^{\text{env}} | \mathbf{a}_t^{\text{rule}}, \mathbf{s}_t) = \pi_{\text{LLM}}(\mathbf{a}^{\text{env}} | \mathbf{p}_t, \mathbf{a}_t^{\text{rule}})$ is the probability of the LLM selecting the environment action \mathbf{a}^{env} .

SAC step The attention-based policy network in Section 4.2 is optimized using the SAC algorithm, which balances reward maximization with exploration by incorporating an entropy term in the objective function. The SAC update process is outlined as follows. First, we define an auxiliary

target value:

$$y = \left(\tilde{r}_t + \gamma \mathbb{E}_{\mathbf{a}_{t+1}^{\text{rule}} \sim \pi_\theta} \left[\min_{j=1,2} \bar{Q}_{\bar{\phi}_j}(\tilde{\mathbf{s}}_{t+1}, \mathbf{a}_{t+1}^{\text{rule}}) - \beta \log \pi_\theta(\mathbf{a}_{t+1}^{\text{rule}} | \mathbf{Q}_{t+1}, \mathbf{k}_{t+1}) \right] \right), \quad (8)$$

The Q-networks are updated by minimizing the loss function:

$$L_Q(\phi_i) = \mathbb{E}_{\mathcal{D}} \left[\left(Q_{\phi_i}(\tilde{\mathbf{s}}_t, \mathbf{a}_t^{\text{rule}}) - y \right)^2 \right], \forall i = 1, 2. \quad (9)$$

The policy network is updated by minimizing the KL divergence between the policy and the Boltzmann distribution induced by Q_ϕ , which is expressed as

$$L_\pi(\theta) = \mathbb{E}_{\mathcal{D}} \left[\beta \log \pi_\theta(\mathbf{a}_t^{\text{rule}} | \mathbf{Q}_{t,t}) - \min_{i=1,2} Q_{\phi_i}(\tilde{\mathbf{s}}_t, \mathbf{a}_t^{\text{rule}}) \right], \quad (10)$$

where β is a temperature parameter. The full SAC update procedure is detailed in Algorithm 3 in Appendix A.1.

5. Experiments & Human Survey

In this section, we evaluate RBRL and empirically show that it can achieve a joint improvement in both reward and explainability over comparable baselines. We briefly summarize these environments here, with additional details in Appendix B.1.

Domains We evaluate RBRL in three environments pertaining to the following two distinct domains:

- **WearableDeviceAssignment**: We use two environments, Uganda and MimicIII, from the vital sign monitoring domain introduced by Boehmer et al. (2024), modeling the allocation of limited wireless devices among postpartum mothers as an restless multi-armed bandit problem (RMAB). Each mother (“arm”) is represented by a state of vital signs (e.g., heart rate, respiratory rate, SPO2) and their variability. Action vector elements are binary: assigning a device to a mother or not. The aim is to prioritize high-risk patients since there are only a limited number of B devices. Rewards penalize abnormal vital signs, with monitoring enabling health-improving interventions. Boehmer et al. (2024) suggests to recast the RMAB problem as an MDP, deciding from which patient to remove a device when a new patient arrives. A penalty is incurred when removing the device from an active patient if there are free devices.
- **HeatAlerts**: We use the `weather2alert` environment from Considine et al. (2025), which formulates issuing heat alerts as a constrained MDP. The action is binary, subject to a constraint on the total number of alerts that can be issued. The state includes the heat index, the remaining budget, and a history of previous alerts. Actions \mathbf{a}_t are binary and represent whether to issue an alert. Rewards are reductions in hospitalizations from the alert. A penalty is incurred when selecting to issue an alert when on budget.

5.1. Environment Reward Optimization

We discuss the main results and refer to Appendix B for the detailed experiment setup. Unless otherwise specified, we use `gpt-4o-mini` (OpenAI, 2024b) as LLM due to its reasonable cost and high performance. All baselines were trained on 3 seeds for 2000 environment steps each.

Q1. Did RBRL optimize the reward function? RBRL is compared to Chain-of-thought (CoT) (Wei et al., 2022) for language reasoning and Proximal Policy Optimization (PPO) (Schulman et al., 2017) for numeric states. Figure 4 indicates RBRL outperforms CoT, showing RL-optimized rule selection improves decision-making. The results show that RBRL exceeds PPO in all environments with equivalent environment steps, suggesting a higher performance when learning in an online setting. For completeness, we also compare against PPO trained at 100k steps, 50 times more. For the `HeatAlerts` environment, RBRL exceeds such asymptotic performance, consistently with the findings of Considine et al. (2025) noting that PPO and other standard RL algorithms struggle to handle the constraints and exploration in this domain. For the `Uganda` and `MimicIII` environments, we observe the trend of RBRL getting closer to 100k PPO, but not reaching the performance. As highlighted in Section 2, various works have remarked that the trade-off between interpretability and performance can be justified to increase system trust, robustness, and adaptability in high-stakes environments.

Q2. Did structured rules help optimization? We conduct two ablation studies on structured rules. First, we benchmark the use of structured rules without RL, called baseline `RulesLLMOnly`, which is shown in Equation (2)-(5). Next, we compare RBRL with a variant optimizing unstructured thoughts, termed thoughts-based RL (TBRL). The implementation mimics RBRL, utilizing a candidate pool \mathcal{R} with the CoT prompt. Results in Figure 5a show that comparing RBRL with `RulesLLMOnly` highlights RL training gains, suggesting rule generation alone does not explain RBRL’s performance. Additionally, significant improvements over TBRL suggest optimizing structured rules is more effective than optimizing free reasoning traces.

Q3. How does RBRL compare to token-level LLM finetuning with RL? We implement LLM finetuning from the environment reward to a Llama 3.1 8B model (Meta AI, 2024), termed `FinetunePPO`. We train a value head on the last hidden states and use KL divergence from the reference model as a regularization reward (Ziegler et al., 2019). A simple CoT generation is used, followed by a call for action question, optimizing the full CoT and action trace. We train 3 seeds for 18 hours on an Nvidia A100 40G GPU, achieving 1200 steps per seed. For compatibility, we also train RBRL on the same Llama 3.1 8B model. Figure 5b compares results, showing a positive but relatively flat trend

RBRL: Joint Explanation and Decision Optimization for Resource Allocation with Language Agents

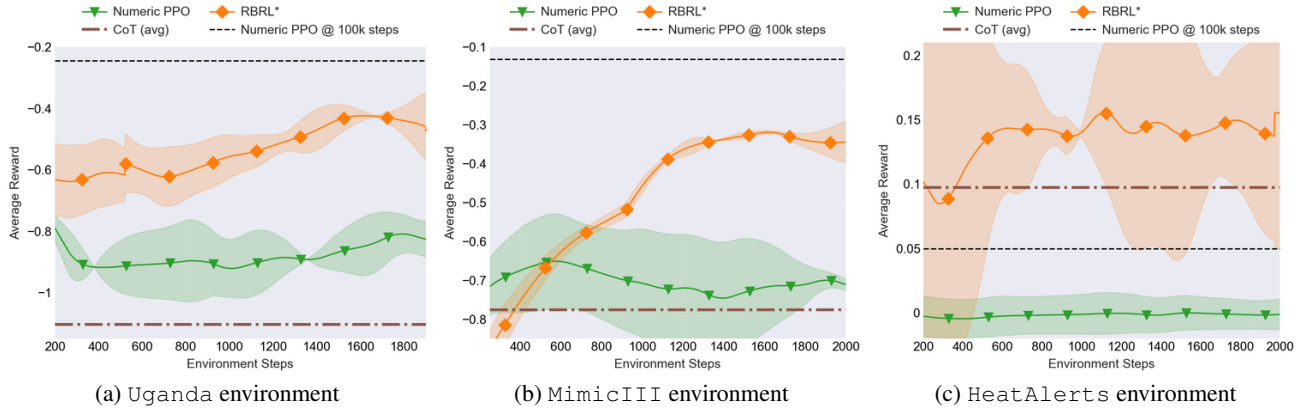


Figure 4: Results from Q1. Main comparison of RBRL on three resource allocation problems. The plots show the mean and standard error across three seeds, using exponentially weighted moving averages with a half-life of 100.

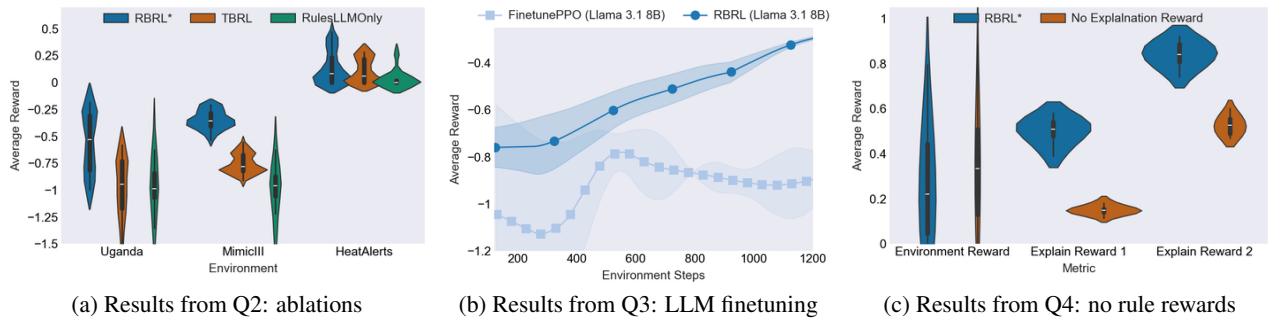


Figure 5: Additional experiments and ablations. (a) Comparison of RBRL with thoughts-based RL (TBRL) and the baseline rule-based LLM without RL training; (b) comparison against LLM finetuning with PPO at the token level from the environment reward with CoT generation for the Mimic environment; (c) shows the effect of removing the rule reward in the HeatAlerts environments. For (a) and (c), we show distribution of rewards in the last 20% training steps.

for finetuning compared to RBRL, suggesting RBRL is better online. Additionally, RBRL runs on a regular laptop, unlike FinetunePPO that needs specialized hardware, and training time for FinetunePPO is about 4x longer on equivalent steps. Due to computation constraints, we only show this experiment for the MimicIII domain, which had the less noise in the previous experiments.

5.2. Human Survey and Explainability

Q4. Did RBRL increase the explainability of post-hoc explanations? A survey with 40 participants was conducted to assess explanation quality, detailed in Appendix E. Each prompt included the task, state, and action space as originally given to the LLM, followed by actions and explanations from the CoT agent and the RBRL agent, without disclosing agent types. Participants were asked to choose preference for explanation A, B, or none. Prompts were split between *Wearable Device Assignment* and *Heat Alerts* domains. Figure 6 shows results, favoring RBRL’s explanations in both domains, with a detailed breakdown in E. An additional experiment with an LLM judge (Gu et al., 2024)

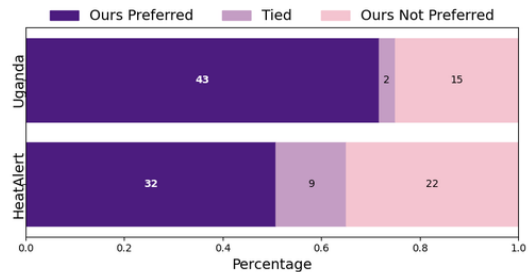


Figure 6: Results from the human survey.

using a large gpt-4o model (OpenAI, 2024a) showed strong agreement with humans, preferring RBRL’s explanations in all but one case.

Q5. What was the effect of the rule reward? During training of RBRL, rules received rewards based on two prompts. We examine an ablation where this reward was omitted. Figure 5c illustrates results for the HeatAlerts environment, noted for high variance and a challenging reward function. We extended training to 5k environment steps to better understand these dynamics. When RBRL is trained without the

rule reward, the environment reward remains steady (with a slight increase), but explainability scores drop significantly. Refer to Section 4.3 for the definition of the rule reward metrics. A decline in metric 1 indicates that rules are less predictive of the optimal actions. A decline in metric 2 suggests rules lack detailed applicability to the current problem state, indicating more generic rather than specialized rule selection. Metric 3 (not shown) was always 1 in all steps, indicating the limitations of directly evaluating post hoc explanations. Although judged by the LLM, these results are encouraging, as our previous experiment showed alignment between the LLM and human assessments.

6. Conclusion

The RBRL framework takes an important step towards addressing the critical challenge of balancing decision efficacy and interpretability in constrained allocation tasks. By synergizing the generative capabilities of LLMs with the optimization power of RL, RBRL introduces a novel paradigm where structured rules, generated dynamically by LLMs, guide RL policies to make transparent and actionable decisions. Evaluations across healthcare and public health domains demonstrate RBRL’s competitive performance against traditional RL baselines while significantly enhancing the quality of human-understandable explanations. Human and LLM-judged surveys further validate that RBRL’s explanations improve trust and clarity, contributing towards addressing the longstanding barrier to deploying AI in high-stakes scenarios.

Impact and Ethics Statement

This work advances the development of transparent AI systems for high-stakes decision-making in domains like healthcare and public policy. By enabling RL agents to generate human-readable rules and explanations, RBRL improves trust and accountability, critical for ethical deployment in settings where lives and resources are at stake.

While the framework prioritizes alignment with human reasoning, potential risks include over-reliance on imperfect LLM-generated rules or explanations that may inadvertently obscure biases in training data. Mitigation requires rigorous validation of rules by domain experts and ongoing monitoring of LLM outputs. Additionally, RBRL’s reliance on LLMs raises computational and accessibility challenges in resource-constrained environments. By addressing these considerations, this research contributes to safer, more equitable AI systems that empower—rather than replace—human decision-makers.

Notice that the Uganda and Heat Alerts datasets used in this study is derived from a simulator provided by [Boehmer et al. \(2024\)](#) and [Considine et al. \(2025\)](#). These simulators do

not include any feature information or identifying details of real patients. Thus, the data generated by the simulator cannot be traced to or represent actual individuals, ensuring privacy and ethical compliance. We emphasize that this is purely a simulated study; and recognize that for any next steps towards real world use, there is a need to conduct rigorous simulation studies on a large scale with real patient data, with detailed assessments of potential biases, verification of policy convergence and its robustness to distribution shifts in patient populations, and making necessary adjustments. Beyond that, there will be a need to obtain ethics and regulatory approval to test the policy in a real-world setting for future comprehensive field-testing, addressing issues of participant consent and privacy; and ultimately there would need to be sufficient human oversight for any future deployment.

Acknowledgments

This work is supported by the Harvard Data Science Initiative, Wadhvani AI, and the National Institutes of Health (R01ES34021, R01ES037156.)

References

- Bahdanau, D., Cho, K., and Bengio, Y. Neural machine translation by jointly learning to align and translate. In *ICLR*, 2015.
- Bhattacharjee, A., Moraffah, R., Garland, J., and Liu, H. Towards llm-guided causal explainability for black-box text classifiers. In *AAAI 2024 Workshop on Responsible Language Models*, 2024.
- Boatin, A. A., Ngonzi, J., Wylie, B. J., Lugobe, H. M., Bebell, L. M., Mugenyi, G., Mohamed, S., Martinez, K., Musinguzi, N., Psaros, C., et al. Wireless versus routine physiologic monitoring after cesarean delivery to reduce maternal morbidity and mortality in a resource-limited setting: protocol of type 2 hybrid effectiveness-implementation study. *BMC Pregnancy and Childbirth*, 21:1–12, 2021.
- Boehmer, N., Zhao, Y., Xiong, G., Rodriguez-Diaz, P., Cibrarian, P. D. C., Ngonzi, J., Boatin, A., and Tambe, M. Optimizing vital sign monitoring in resource-constrained maternal care: An rl-based restless bandit approach. *arXiv preprint arXiv:2410.08377*, 2024.
- Carta, T., Romac, C., Wolf, T., Lamprier, S., Sigaud, O., and Oudeyer, P.-Y. Grounding large language models in interactive environments with online reinforcement learning. In *ICML*, 2023.
- Colas, C., Karch, T., Moulin-Frier, C., and Oudeyer, P.-Y. Language and culture internalization for human-like

- autotelic ai. *Nature Machine Intelligence*, 4(12):1068–1076, 2022.
- Considine, E. M., Nethery, R. C., Wellenius, G. A., Dominici, F., and Tec, M. Optimizing heat alert issuance with reinforcement learning. In *AAAI*, 2025.
- CSL. Senate bill no. 896: Generative artificial intelligence accountability act. <https://legiscan.com/CA/text/SB896/id/3023382>, 2024. Accessed: 2025-02-06.
- Das, D., Chernova, S., and Kim, B. State2explanation: Concept-based explanations to benefit agent learning and user understanding. *NeurIPS*, 2023.
- Doshi-Velez, F. and Kim, B. Towards a rigorous science of interpretable machine learning. *arXiv preprint arXiv:1702.08608*, 2017.
- Du, Y., Watkins, O., Wang, Z., Colas, C., Darrell, T., Abbeel, P., Gupta, A., and Andreas, J. Guiding pretraining in reinforcement learning with large language models. In *ICML*, pp. 8657–8677, 2023.
- DuBois, K. N. Deep medicine: How artificial intelligence can make healthcare human again. *Perspectives on Science and Christian Faith*, 71(3):199–201, 2019.
- EPC. Regulation (eu) 2024/1689 of the european parliament and of the council of 13 june 2024 laying down harmonised rules on artificial intelligence. <http://data.europa.eu/eli/reg/2024/1689/oj>, 2024. Accessed: 2025-02-06.
- Feng, X., Wan, Z., Fu, H., Liu, B., Yang, M., Koushik, G. A., Hu, Z., Wen, Y., and Wang, J. Natural language reinforcement learning. *arXiv preprint arXiv:2411.14251*, 2024.
- Furuta, H., Matsuo, Y., Faust, A., and Gur, I. Exposing limitations of language model agents in sequential-task compositions on the web. In *ICLR 2024 Workshop on Large Language Model (LLM) Agents*, 2024.
- Gebrael, G., Sahu, K. K., Chigarira, B., Tripathi, N., Mathew Thomas, V., Sayegh, N., Maughan, B. L., Agarwal, N., Swami, U., and Li, H. Enhancing triage efficiency and accuracy in emergency rooms for patients with metastatic prostate cancer: a retrospective analysis of artificial intelligence-assisted triage using chatgpt 4.0. *Cancers*, 15(14):3717, 2023.
- Gu, J., Jiang, X., Shi, Z., Tan, H., Zhai, X., Xu, C., Li, W., Shen, Y., Ma, S., Liu, H., et al. A survey on llm-as-a-judge. *arXiv preprint arXiv:2411.15594*, 2024.
- Haarnoja, T., Zhou, A., Abbeel, P., and Levine, S. Soft actor-critic: Off-policy maximum entropy deep reinforcement learning with a stochastic actor. In *Proceedings of the 35th International Conference on Machine Learning*, pp. 1856–1865. PMLR, 2018.
- Hoffman, R. R., Mueller, S. T., Klein, G., and Litman, J. Metrics for explainable ai: Challenges and prospects. *arXiv preprint arXiv:1812.04608*, 2018.
- Hu, E. J., Shen, Y., Wallis, P., Allen-Zhu, Z., Li, Y., Wang, S., Wang, L., and Chen, W. Lora: Low-rank adaptation of large language models. *arXiv preprint arXiv:2106.09685*, 2021.
- Hu, H. and Sadigh, D. Language instructed reinforcement learning for human-ai coordination. In *ICML*, 2023.
- Huang, S., Dossa, R. F. J., Ye, C., Braga, J., Chakraborty, D., Mehta, K., and ao G.M. Araújo, J. Cleanrl: High-quality single-file implementations of deep reinforcement learning algorithms. *Journal of Machine Learning Research*, 23(274):1–18, 2022. URL <http://jmlr.org/papers/v23/21-1342.html>.
- Johnson, A. E., Pollard, T. J., Shen, L., Lehman, L.-w. H., Feng, M., Ghassemi, M., Moody, B., Szolovits, P., Anthony Celi, L., and Mark, R. G. Mimic-iii, a freely accessible critical care database. *Scientific data*, 3(1):1–9, 2016.
- Likmeta, A., Metelli, A. M., Tirinzoni, A., Giol, R., Restelli, M., and Romano, D. Combining reinforcement learning with rule-based controllers for transparent and general decision-making in autonomous driving. *Robotics and Autonomous Systems*, 131:103568, 2020.
- Meta AI. Introducing llama 3.1: Our most capable models to date. *AI at Meta*, 2024. URL <https://ai.meta.com/blog/meta-llama-3-1/>.
- Milani, S., Topin, N., Veloso, M., and Fang, F. Explainable reinforcement learning: A survey and comparative review. *ACM Computing Surveys*, 56(7):1–36, 2024.
- OpenAI. GPT-4o system card. *arXiv preprint arXiv:2410.21276*, 2024a. URL <https://arxiv.org/abs/2410.21276>.
- OpenAI. Gpt-4o mini: Advancing cost-efficient intelligence. *OpenAI Blog*, 2024b.
- Park, J. S., O’Brien, J., Cai, C. J., Morris, M. R., Liang, P., and Bernstein, M. S. Generative agents: Interactive simulacra of human behavior. In *Proceedings of the 36th annual acm symposium on user interface software and technology*, pp. 1–22, 2023.

- Peng, X., Riedl, M., and Ammanabrolu, P. Inherently explainable reinforcement learning in natural language. In Oh, A. H., Agarwal, A., Belgrave, D., and Cho, K. (eds.), *NeurIPS*, 2022.
- Poeta, E., Ciravegna, G., Pastor, E., Cerquitelli, T., and Baralis, E. Concept-based explainable artificial intelligence: A survey. *arXiv preprint arXiv:2312.12936*, 2023.
- Putta, P., Mills, E., Garg, N., Motwani, S., Finn, C., Garg, D., and Rafailov, R. Agent q: Advanced reasoning and learning for autonomous ai agents. *arXiv preprint arXiv:2408.07199*, 2024.
- Rashid, A., Wu, R., Grosse, J., Kristiadi, A., and Poupart, P. A critical look at tokenwise reward-guided text generation. *arXiv preprint arXiv:2406.07780*, 2024.
- Reimers, N. and Gurevych, I. Sentence-bert: Sentence embeddings using siamese bert-networks. In *Proceedings of the 2019 Conference on EMNLP-IJCNLP*, pp. 3980–3990. Association for Computational Linguistics, 2019.
- Rudin, C. Stop explaining black box machine learning models for high stakes decisions and use interpretable models instead. *Nature machine intelligence*, 1(5):206–215, 2019.
- Schulman, J., Wolski, F., Dhariwal, P., Radford, A., and Klimov, O. Proximal policy optimization algorithms. *arXiv preprint arXiv:1707.06347*, 2017.
- Shen, Y., McClosky, B., and Zavlanos, M. Multi-agent reinforcement learning for resource allocation in large-scale robotic warehouse sortation centers. 2023.
- Shen, Y., John, A. E. A., and Fain, B. Explainable rewards in RLHF using LLM-as-a-judge, 2024. URL <https://openreview.net/forum?id=FaOeBrlPst>.
- Shevtsova, D., Ahmed, A., Boot, I. W., Sanges, C., Hudecek, M., Jacobs, J. J., Hort, S., Vrijhoef, H. J., et al. Trust in and acceptance of artificial intelligence applications in medicine: Mixed methods study. *JMIR Human Factors*, 11(1):e47031, 2024.
- Sinclair, S. R., Vieira Frujeri, F., Cheng, C.-A., Marshall, L., Barbalho, H., Li, J., Neville, J., Menache, I., and Swaminathan, A. Hindsight learning for mdps with exogenous inputs. In *ICML*, 2023.
- Singh, C., Inala, J. P., Galley, M., Caruana, R., and Gao, J. Rethinking interpretability in the era of large language models. *arXiv preprint arXiv:2402.01761*, 2024.
- Srivastava, M., Colas, C., Sadigh, D., and Andreas, J. Policy learning with a language bottleneck. In *RLC Workshop on Training Agents with Foundation Models*, 2024.
- Sumers, T., Yao, S., Narasimhan, K., and Griffiths, T. Cognitive architectures for language agents. *TMLR*, 2024. URL <https://openreview.net/forum?id=1i6ZCvflQJ>.
- Szot, A., Schwarzer, M., Agrawal, H., Mazouze, B., Metcalf, R., Talbott, W., Mackraz, N., Hjelm, R. D., and Toshev, A. T. Large language models as generalizable policies for embodied tasks. In *ICLR*, 2023.
- Talaat, F. M. Effective deep q-networks (edqn) strategy for resource allocation based on optimized reinforcement learning algorithm. *Multimedia Tools and Applications*, 81(28):39945–39961, 2022.
- Tan, W., Zhang, W., Liu, S., Zheng, L., Wang, X., and An, B. True knowledge comes from practice: Aligning large language models with embodied environments via reinforcement learning. In *ICLR*, 2024.
- Together AI. Announcing function calling and json mode, 2024. URL <https://www.together.ai/blog/function-calling-json-mode>. Accessed: 2025-01-30.
- Towers, M., Kwiatkowski, A., Terry, J. K., Balis, J. U., De Cola, G., Deleu, T., Goulão, M., Kallinteris, A., Krimmel, M., KG, A., et al. Gymnasium: A standard interface for reinforcement learning environments. *arXiv preprint arXiv:2407.17032*, 2024. URL <https://arxiv.org/abs/2407.17032>.
- Vaswani, A., Shazeer, N., Parmar, N., Uszkoreit, J., Jones, L., Gomez, A. N., Kaiser, K., and Polosukhin, I. Attention is all you need. In *Advances in Neural Information Processing Systems*, volume 30, 2017.
- Vezhnevets, A. S., Agapiou, J. P., Aharon, A., Ziv, R., Matyas, J., Duñez-Guzmán, E. A., Cunningham, W. A., Osindero, S., Karmon, D., and Leibo, J. Z. Generative agent-based modeling with actions grounded in physical, social, or digital space using concordia. *arXiv preprint arXiv:2312.03664*, 2023.
- Wang, Z., Cai, S., Chen, G., Liu, A., Ma, X., Liang, Y., and CraftJarvis, T. Describe, explain, plan and select: interactive planning with large language models enables open-world multi-task agents. In *NeurIPS*, 2023.
- Waytowich, N. R., White, D., Sunbeam, M., and Goecks, V. G. Atari-gpt: Investigating the capabilities of multimodal large language models as low-level policies for atari games. *arXiv preprint arXiv:2408.15950*, 2024.
- Wei, J., Wang, X., Schuurmans, D., Bosma, M., Xia, F., Chi, E., Le, Q. V., Zhou, D., et al. Chain-of-thought prompting elicits reasoning in large language models. *Advances in neural information processing systems*, 35:24824–24837, 2022.

- Wen, M., Wan, Z., Wang, J., Zhang, W., and Wen, Y. Reinforcing LLM agents via policy optimization with action decomposition. In *The Thirty-eighth Annual Conference on Neural Information Processing Systems*, 2024.
- Whittle, P. Restless bandits: Activity allocation in a changing world. *Journal of applied probability*, 25(A):287–298, 1988.
- Wolf, T., Debut, L., Sanh, V., Chaumond, J., Delangue, C., Moi, A., Cistac, P., Rault, T., Louf, R., Funtowicz, M., Davison, J., Shleifer, S., von Platen, P., Ma, C., Jernite, Y., Plu, J., Xu, C., Le Scao, T., Gugger, S., Drame, M., Lhoest, Q., and Rush, A. M. Transformers: State-of-the-art natural language processing. In *Proceedings of the 2020 Conference on Empirical Methods in Natural Language Processing: System Demonstrations*, pp. 38–45, Online, October 2020. Association for Computational Linguistics. URL <https://www.aclweb.org/anthology/2020.emnlp-demos.6>.
- Xi, Z., Ding, Y., Chen, W., Hong, B., Guo, H., Wang, J., Yang, D., Liao, C., Guo, X., He, W., et al. Agentgym: Evolving large language model-based agents across diverse environments. *arXiv preprint arXiv:2406.04151*, 2024.
- Xiong, G., Qin, X., Li, B., Singh, R., and Li, J. Index-aware reinforcement learning for adaptive video streaming at the wireless edge. In *Proceedings of the Twenty-Third International Symposium on Theory, Algorithmic Foundations, and Protocol Design for Mobile Networks and Mobile Computing*, pp. 81–90, 2022.
- Xiong, G., Wang, S., Yan, G., and Li, J. Reinforcement learning for dynamic dimensioning of cloud caches: A restless bandit approach. *IEEE/ACM Transactions on Networking*, 31(5):2147–2161, 2023.
- Yao, S., Zhao, J., Yu, D., Du, N., Shafran, I., Narasimhan, K. R., and Cao, Y. React: Synergizing reasoning and acting in language models. In *ICLR*, 2023.
- Yu, C., Liu, J., Nemati, S., and Yin, G. Reinforcement learning in healthcare: A survey. *ACM Computing Surveys (CSUR)*, 55(1):1–36, 2021.
- Yu, Y., Yao, Z., Li, H., Deng, Z., Cao, Y., Chen, Z., Suchow, J. W., Liu, R., Cui, Z., Xu, Z., et al. Fincon: A synthesized llm multi-agent system with conceptual verbal reinforcement for enhanced financial decision making. *arXiv preprint arXiv:2407.06567*, 2024.
- Zhai, Y., Bai, H., Lin, Z., Pan, J., Tong, S., Zhou, Y., Suhr, A., Xie, S., LeCun, Y., Ma, Y., et al. Fine-tuning large vision-language models as decision-making agents via reinforcement learning. *arXiv preprint arXiv:2405.10292*, 2024.
- Zhang, X., Guo, Y., Stepputtis, S., Sycara, K., and Campbell, J. Understanding your agent: Leveraging large language models for behavior explanation. *arXiv preprint arXiv:2311.18062*, 2023.
- Zhao, Y., Behari, N., Hughes, E., Zhang, E., Nagaraj, D., Tuyls, K., Taneja, A., and Tambe, M. Towards a pre-trained model for restless bandits via multi-arm generalization. In *Proc. of IJCAI*, pp. 321–329, 2024.
- Ziegler, D. M., Stiennon, N., Wu, J., Brown, T. B., Radford, A., Amodei, D., Christiano, P., and Irving, G. Fine-tuning language models from human preferences. *arXiv preprint arXiv:1909.08593*, 2019.

A. Algorithmic and Mathematical Details

A.1. Algorithms

In this subsection, we present the detailed pseudocodes for `Rule_Search` in Algorithm 2 and the SAC for attention-based policy network in Algorithm 3.

Algorithm 2 `Rule_Search`: Rule Selection via Attention-Based Policies

Require: Numeric state representation $\mathbf{s}_t \in \mathbb{R}^{d_s}$ and rule set $\mathcal{R}_t = \{\boldsymbol{\rho}_i^t\}_{i=1}^q$. Hidden dimension d_h .

- 1: Embed each rule $\boldsymbol{\rho}_i^t \in \mathcal{R}_t$ into a numeric vector using sentence embeddings $\mathbf{q}_i^t = \text{embed}(\boldsymbol{\rho}_i^t) \in \mathbb{R}^{d_h}$ (e.g., Sentence-BERT) and stack to form a query matrix $\mathbf{Q}_t \in \mathbb{R}^{d_h \times q}$. // *Rule Candidate Embedding*
 - 2: The state \mathbf{s}_t is projected by a linear layer with SiLU activation: $\mathbf{k}_t = \text{SiLU}(\text{Linear}(\mathbf{s}_t)) \in \mathbb{R}^{d_h}$, with d_h being to denote the architecture hidden dimension. // *State Representation*
 - 3: Use cross-attention to obtain $\mathbf{h} = \text{CrossAttention}(\mathbf{Q}_t, \mathbf{k}_t, \mathbf{k}_t) \in \mathbb{R}^{q \times d_h}$.
 - 4: (Optional) Further apply a self-attention network $\mathbf{h} \leftarrow \text{SelfAttention}(\mathbf{h})$.
 - 5: Apply linear layer to obtain logits vector $\boldsymbol{\alpha}_\theta^t = \text{Linear}(\mathbf{h}) \in \mathbb{R}^{q \times 1}$.
 - 6: Calculate the policy distribution: $\pi_{\theta,i}(\mathbf{Q}_t, \mathbf{k}_t) = \frac{\exp(\alpha_{\theta,i}^t(\mathbf{Q}_t, \mathbf{k}_t))}{\sum_{j=1}^q \exp(\alpha_{\theta,j}^t(\mathbf{Q}_t, \mathbf{k}_t))}$, where $\alpha_{\theta,i}^t$ is i -th element in $\boldsymbol{\alpha}_\theta^t$.
 - 7: Sample rule $\mathbf{a}_t^{\text{rule}} \sim \text{Categorical}(\mathcal{R}; (\pi_{\theta,i}(\mathbf{Q}_t, \mathbf{k}_t))_{i=1}^q)$. // *Rule Selection with Attention*
 - 8: **Return** $\mathbf{a}_t^{\text{rule}}$.
-

Algorithm 2 outlines the process of rule selection using attention-based policies. First, each rule candidate $\boldsymbol{\rho}_i^t$ is embedded into a numeric vector \mathbf{q}_i^t using a sentence embedding technique (e.g., Sentence-BERT), forming a query matrix \mathbf{Q}_t . The state \mathbf{s}_t is also converted into a numeric vector \mathbf{k}_t . Cross-attention is applied between \mathbf{Q}_t and \mathbf{k}_t to generate an attention representation \mathbf{h} , which may optionally be refined using a self-attention mechanism. A linear layer processes \mathbf{h} to produce score vector $\boldsymbol{\alpha}_\theta^t$. These scores define the policy distribution π_θ , from which a rule $\mathbf{a}_t^{\text{rule}}$ is sampled. This attention-based approach ensures efficient selection of rules by leveraging contextual relationships between the state and rule candidates.

Algorithm 3 SAC for Attention-based Policy Network

- 1: Initialize Q networks Q_{ϕ_1}, Q_{ϕ_2} and policy network π_θ with random parameters ϕ_1, ϕ_2, θ .
 - 2: Initialize target Q networks $\bar{Q}_{\bar{\phi}_1}, \bar{Q}_{\bar{\phi}_2}$ with weights $\bar{\phi}_1 \leftarrow \phi_1, \bar{\phi}_2 \leftarrow \phi_2$.
 - 3: Initialize temperature parameter β and target entropy $\mathcal{H}_{\text{target}}$; Initialize replay buffer \mathcal{D} .
 - 4: **for** episode = 1, ..., M **do**
 - 5: Initialize environment and observe initial state $\tilde{\mathbf{s}}_1$.
 - 6: **for** step $t = 1, \dots, T$ **do**
 - 7: Sample action $\mathbf{a}_t^{\text{rule}} \sim \pi_\theta(\cdot | \tilde{\mathbf{s}}_t)$.
 - 8: Execute action $\mathbf{a}_t^{\text{rule}}$, observe reward \tilde{r}_t and next state $\tilde{\mathbf{s}}_{t+1}$.
 - 9: Store transition $(\tilde{\mathbf{s}}_t, \mathbf{a}_t^{\text{rule}}, \tilde{r}_t, \tilde{\mathbf{s}}_{t+1})$ in replay buffer \mathcal{D} .
 - 10: **if** enough samples in \mathcal{D} **then**
 - 11: Sample a mini-batch of transitions $(\tilde{\mathbf{s}}_t, \mathbf{a}_t^{\text{rule}}, \tilde{r}_t, \tilde{\mathbf{s}}_{t+1})$ from \mathcal{D} .
 - 12: Compute target Q values: $y_t = \tilde{r}_t + \gamma \mathbb{E}_{\mathbf{a}_{t+1}^{\text{rule}} \sim \pi_\theta(\cdot | \tilde{\mathbf{s}}_{t+1})} \left[\min_{j=1,2} \bar{Q}_{\bar{\phi}_j}(\tilde{\mathbf{s}}_{t+1}, \mathbf{a}_{t+1}^{\text{rule}}) - \alpha \log \pi_\theta(\mathbf{a}_{t+1}^{\text{rule}} | \tilde{\mathbf{s}}_{t+1}) \right]$.
 - 13: Update Q networks by minimizing:
 - 14: $L_Q(\phi_i) = \mathbb{E}_{(\tilde{\mathbf{s}}_t, \mathbf{a}_t^{\text{rule}}, \tilde{r}_t, \tilde{\mathbf{s}}_{t+1})} \left[(Q_{\phi_i}(\tilde{\mathbf{s}}_t, \mathbf{a}_t^{\text{rule}}) - y_t)^2 \right]$ for $i = 1, 2$.
 - 15: Update policy network by minimizing:
 - 16: $L_\pi(\theta) = \mathbb{E}_{\tilde{\mathbf{s}}_t, \mathbf{a}_t^{\text{rule}} \sim \pi_\theta} \left[\beta \log \pi_\theta(\mathbf{a}_t^{\text{rule}} | \tilde{\mathbf{s}}_t) - \min_{j=1,2} Q_{\phi_j}(\tilde{\mathbf{s}}_t, \mathbf{a}_t^{\text{rule}}) \right]$.
 - 17: Update temperature parameter by minimizing:
 - 18: $L_\beta(\beta) = \mathbb{E}_{\tilde{\mathbf{s}}_t, \mathbf{a}_t^{\text{rule}} \sim \pi_\theta} \left[-\beta (\log \pi_\theta(\mathbf{a}_t^{\text{rule}} | \tilde{\mathbf{s}}_t) + \mathcal{H}_{\text{target}}) \right]$.
 - 19: Update target Q networks:
 - 20: $\bar{\phi}_i \leftarrow \tau \phi_i + (1 - \tau) \bar{\phi}_i$ for $i = 1, 2$.
 - 21: **end if**
 - 22: **end for**
 - 23: **end for**
-

Algorithm 3 presents the SAC algorithm tailored for training an attention-based policy network in selecting the desired rule. This method combines entropy-regularized policy optimization with a structured approach to handle rule-selection effectively. The algorithm begins with the initialization of key components: Q networks Q_{ϕ_1}, Q_{ϕ_2} , target Q networks $\bar{Q}_{\phi_1}, \bar{Q}_{\phi_2}$, and a policy network π_θ . Random parameters are assigned to these networks, and the target Q networks are synchronized with the initial Q networks. A temperature parameter α is initialized to regulate the entropy \mathcal{H}_{target} in the policy objective, ensuring a balance between exploration and exploitation. A replay buffer \mathcal{D} is set up to store transition data. Notice the entropy is defined as

$$\mathcal{H}_{target} = - \sum_{i=1}^q \pi_\theta(\mathbf{a}_t^{\text{rule}} | \mathbf{k}_t, \mathbf{Q}_t) \log \pi_\theta(\mathbf{a}_t^{\text{rule}} | \mathbf{k}_t, \mathbf{Q}_t). \quad (11)$$

During training, each episode starts with the initialization of the environment, and the agent observes the initial state $\tilde{\mathbf{s}}_1$. At every time step, the policy network generates an action $\mathbf{a}_t^{\text{rule}}$ based on the current state. This action is executed in the environment, resulting in a reward \tilde{r}_t and a state transition to $\tilde{\mathbf{s}}_{t+1}$. These transitions are stored in the replay buffer for optimization. When sufficient transitions are available in the buffer, the algorithm samples a mini-batch of transitions and computes the target Q values. The target Q values incorporate entropy regularization and are computed using the minimum of the target Q networks to ensure stability. The Q networks are updated by minimizing the mean squared error between the predicted Q values and the computed targets. The policy network is optimized by minimizing a loss function that combines the policy entropy with the expected Q value, ensuring a stochastic and exploratory policy. The temperature parameter β is updated to maintain the desired balance between exploration and exploitation. Finally, the target Q networks are softly updated to stabilize training. This iterative process continues across episodes and time steps, progressively refining the policy network to achieve optimal rule selection.

A.2. Proof of Theorem 4.1

In this section, we provide the detailed proofs for Theorem 4.1. We start with the following equation

$$\begin{aligned} & P(\mathcal{R}_{t+1} | \mathbf{s}_{t+1}) \cdot \int_a P(\mathbf{s}_{t+1} | \mathbf{a}^{\text{env}}, \mathbf{s}_t) \cdot P(\mathbf{a}^{\text{env}} | \mathbf{a}_t^{\text{rule}}, \mathbf{s}_t) d\mathbf{a}^{\text{env}} \\ &= P(\mathcal{R}_{t+1} | \mathbf{s}_{t+1}) \cdot \underbrace{\int_a P(\mathbf{s}_{t+1} | \mathbf{a}^{\text{env}}, \mathbf{s}_t, \mathcal{R}_t, \mathbf{a}_t^{\text{rule}}) \cdot P(\mathbf{a}^{\text{env}} | \mathcal{R}_t, \mathbf{a}_t^{\text{rule}}, \mathbf{s}_t) d\mathbf{a}^{\text{env}}}_{(a) P(\mathbf{s}_{t+1} | \mathbf{a}^{\text{env}}, \mathbf{s}_t, \mathcal{R}_t, \mathbf{a}_t^{\text{rule}}) = P(\mathbf{s}_{t+1} | \mathbf{a}^{\text{env}}, \mathbf{s}_t)} \\ &= P(\mathcal{R}_{t+1} | \mathbf{s}_{t+1}) \cdot \underbrace{\int_a P(\mathbf{s}_{t+1} | \mathbf{a}^{\text{env}}, \mathbf{s}_t, \mathcal{R}_t, \mathbf{a}_t^{\text{rule}}) \cdot P(\mathbf{a}^{\text{env}} | \mathbf{s}_t, \mathcal{R}_t, \mathbf{a}_t^{\text{rule}}) d\mathbf{a}^{\text{env}}}_{(b) P(\mathbf{a}^{\text{env}} | \mathbf{s}_t, \mathcal{R}_t, \mathbf{a}_t^{\text{rule}}) = P(\mathbf{a}^{\text{env}} | \mathcal{R}_t, \mathbf{a}_t^{\text{rule}})} \\ &= P(\mathcal{R}_{t+1} | \mathbf{s}_{t+1}) \cdot \underbrace{\int_a P(\mathbf{s}_{t+1}, \mathbf{a}^{\text{env}} | \mathbf{s}_t, \mathcal{R}_t, \mathbf{a}_t^{\text{rule}}) d\mathbf{a}^{\text{env}}}_{P(A|B,C) \cdot P(B|C) = P(A,B|C)} \\ &= P(\mathcal{R}_{t+1} | \mathbf{s}_{t+1}) \cdot P(\mathbf{s}_{t+1} | \mathbf{s}_t, \mathcal{R}_t, \mathbf{a}_t^{\text{rule}}) \\ &= \underbrace{P(\mathcal{R}_{t+1} | \mathbf{s}_{t+1}, \mathbf{s}_t, \mathcal{R}_t, \mathbf{a}_t^{\text{rule}})}_{(c) P(\mathcal{R}_{t+1} | \mathbf{s}_{t+1}, \mathbf{s}_t, \mathcal{R}_t, \mathbf{a}_t^{\text{rule}}) = P(\mathcal{R}_{t+1} | \mathbf{s}_{t+1})} \cdot P(\mathbf{s}_{t+1} | \mathbf{s}_t, \mathcal{R}_t, \mathbf{a}_t^{\text{rule}}) \\ &= \underbrace{P(\mathbf{s}_{t+1}, \mathcal{R}_{t+1} | \mathbf{s}_t, \mathcal{R}_t, \mathbf{a}_t^{\text{rule}})}_{P(A|B,C) \cdot P(B|C) = P(A,B|C)} \\ &= \underbrace{P(\tilde{\mathbf{s}}_{t+1} | \tilde{\mathbf{s}}_t, \mathbf{a}_t^{\text{rule}})}_{\tilde{\mathbf{s}}_t := (\mathbf{s}_t, \mathcal{R}_t)}, \end{aligned} \quad (12)$$

where (a) follows from the fact that the transition to \mathbf{s}_{t+1} is fully determined by current state \mathbf{s}_t and current action to the environment $\mathbf{a}_t^{\text{env}}$, i.e., independent on rule set \mathcal{R}_t and selected rule $\mathbf{a}_t^{\text{rule}}$; (b) holds since $\mathbf{a}_t^{\text{env}}$ is determined only by the selected rule $\mathbf{a}_t^{\text{rule}}$ and the state \mathbf{s}_t ; (c) is due to our designed rule generation procedure where \mathcal{R}_{t+1} is generated by the LLM from the the latest state \mathbf{s}_{t+1} . This completes the proof.

B. Experiment Setup

B.1. Environments Details

B.1.1. WEARABLE DEVICE ASSIGNMENT DOMAIN

The simulator for the Uganda domain is adapted from (Boehmer et al., 2024) with minor modifications to simplify the problem. This section provides an overview of the environment, with additional details available in the original paper. In this environment, they want to allocate vital sign monitoring devices to mothers arriving in a maternal unit in order to better monitor mothers’ health condition. Each mother’s state is modeled by her vital signs (heart rate, respiratory rate, and blood oxygen saturation) along with each vital sign’s variability. The mother’s vital sign transition is governed by a multivariate Gaussian distribution defined over her vital signs at the current timestep and next timestep, learned from de-identified vital sign data collected from patients at Mbarara Regional Referral Hospital. MIMIC-III (Johnson et al., 2016) is another de-identified clinical vital sign dataset that includes the same set of vital signs as the Uganda domain. The key difference is they have different data sources, as MIMIC-III’s data comes from Beth Israel Deaconess Medical Center in Boston.

Wearing a monitoring device does not directly alter a mother’s vital sign trajectory but has an indirect positive effect by triggering alerts when vital signs deviate from the normal range. These alerts often lead to medical interventions that improve the mother’s condition. If no monitoring device is assigned (passive action), the mother’s next state is sampled from the multivariate Gaussian distribution conditioned on the current state. If a monitoring device is assigned and the vital signs remain within the normal range, the vital signs evolve as under the passive action. However, if any vital sign deviates from the normal range, there is a 30% chance the vital signs evolve as under the passive action, based on empirical evidence suggesting that clinicians fail to respond in such cases 30% of the time (Boatin et al., 2021). Otherwise, vital signs are probabilistically adjusted towards the normal range before sampling the next state, modeling the positive impact of medical intervention.

The algorithm’s goal is to optimize monitoring device allocation to maximize the aggregate reward across all mothers. We simplify the problem by requiring exactly one new mother to join the maternal unit at each timestep, starting with a single mother in the unit. The system has a budget of five monitoring devices. A device must be allocated to the new mother, and if all devices are already in use, one must be removed from a current user. Once removed, a device cannot be reassigned to the same mother. Each mother remains in the maternal unit for 10 timesteps, after which her vital sign trajectory no longer contributes to the reward. Once a device is taken from a mother, we directly sample her entire vital sign trajectory under passive action for the remaining timesteps she stays in the maternal unit and compute all her future rewards. We can directly compute future rewards because the mother will not receive the device again, so she will only undergo passive action in the remaining time. This observation enables us to maintain a smaller observation space, as we only need to keep track of the states of the mothers who own the device.

In this domain, the constraints can be written as $\|\mathbf{a}_t \in \mathcal{R}^{d_2}\|_1 \leq B, \forall t$, which d_2 represents the number of patients in the system at each time slot, and the 1-norm of the action vector must remain within the budget B .

B.1.2. HEAT ALERTS DOMAIN

The heat alert issuance problem can be modeled as an MDP in the context of RL (Considine et al., 2025). The state at any given time, denoted as \mathbf{s}_t , encompasses both exogenous and endogenous factors. Exogenous factors include current weather conditions, such as the heat index, temperature, and humidity, which directly influence the risk of heat-related health issues. Endogenous factors include the history of issued alerts, such as the number and timing of past alerts, their effectiveness, and the remaining budget for the season. Additionally, the day of the week is considered, as public responsiveness to alerts may vary between weekdays and weekends. The action space is binary, with $\mathbf{a}_t \in \mathbb{Z}_2$. The decision to issue a heatwave alert $\mathbf{a}_t = 1$ or not $\mathbf{a}_t = 0$ is constrained by the remaining alert budget. If the budget is exhausted, no further alerts can be issued. The reward function is designed to reflect the reduction in heat-related hospitalizations, which depends on the effectiveness of the alert under current weather conditions. A Bayesian hierarchical framework could be employed to model the health impact of alerts, capturing the uncertainty in their effectiveness. Importantly, consecutive alerts tend to lose effectiveness, introducing a diminishing returns effect that must be accounted for in the decision-making process.

The transition dynamics, $P(\mathbf{s}_{t+1}|\mathbf{s}_t, \mathbf{a}_t)$, describe how the system evolves over time. The next state is influenced by weather trajectories, the action taken, and public responsiveness to alerts. For instance, issuing an alert reduces the remaining budget and updates the history of issued alerts, while the weather conditions may change independently. Public responsiveness may also vary based on the frequency and timing of past alerts. A key constraint in this problem is the limited alert budget,

which necessitates strategic allocation of alerts throughout the season. The goal is to learn a policy $\pi(\mathbf{s}_t|\mathbf{a}_t)$ that maximizes cumulative rewards by effectively issuing alerts during severe heat conditions to minimize hospitalizations, while conserving the budget for future use. This involves balancing immediate health benefits against the potential need for alerts later in the season, addressing the trade-offs between short-term and long-term outcomes.

For this domain, the budget constraints can be expressed as $\sum_{t=1}^h \mathbf{a}_t \in \mathbb{R} \leq B$, where the total sum of all actions over time horizon h must not exceed a budget threshold B .

B.2. Gym environments an Language Wrappers

We implemented the `WearableDevicesAssignment` environments as gymnasium environments (Towers et al., 2024), while the `HeatAlerts` domain was already available in this format. We additionally created a `LanguageWrapper` Python class described in Table 1, which can be applied to any gymnasium environment. Our code implementations can be applied to any environment wrapped in this class.

Method/Property	Type	Description
<code>task.text</code>	Property (Abstract)	Returns a description of the task that the environment is solving.
<code>action.space.text</code>	Property (Abstract)	Returns a description of the action space of the environment.
<code>state.descriptor(obs, info)</code>	Abstract Method	Converts the observation into a text description.
<code>step(action)</code>	Method	Wraps the step method of the environment adding the text representation to the state space.
<code>reset(seed, options)</code>	Method	Wraps the reset method of the environment adding the text representation to the state space.
<code>action.parser(s)</code>	Method	Parses an action string and converts it into an appropriate format for the environment's action space.
<code>(rule.examples</code>	Property (Optional)	Returns a list of string representation of rules.

Table 1: Methods and properties of the `LanguageWrapper` class

B.3. RL implementations, hyperparameters and Settings

We implemented three main RL algorithms for the experiment sections: Attention-based SAC for RBRL, numeric PPO, and Finetuning-based PPO. We based our implementation on the single-file, high-quality implementations from the `cleanrl` project (Huang et al., 2022). For Attention-based SAC, we required significant changes to keep track of the rule-augmented state space, as described in Section 4.4. Other major changes to the baseline SAC implementation (originally designed for Atari) were more frequent target network updates and updating the actor and critic four times per iteration. This was done to improve sample efficiency and cope with the slow generation by the LLM. Numeric PPO was used practically without modification.

For the Finetuning-based PPO, we used low-rank adaptation (LoRA) (Hu et al., 2021) with the Transformers package and models hosted on Llama Hugging Face (Wolf et al., 2020). We set the rank to $r = 1$ and the adaptation weight to 2, resulting in only 0.8% trainable parameters (still an order of magnitude larger than the Attention-based policy). Tables 2, 3, and 4 show the hyperparameters and settings used in these implementations.

B.4. Computing environment

SAC attention can run on a regular laptop since most of the computation happens in the cloud through API LLM calls, while the RL module is small and can run on personal CPUs. Nonetheless, the process is bottlenecked by the speed of generation from the APIs. A full run of 2 million environment steps, with parallelized API calls across four environments, took approximately four hours to complete. One training cycle did not exceed \$10 in API costs. However, all the experiments and development incurred approximately \$1,500 in API costs. As described in the main text, the LLM fine-tuning experiments used an Nvidia A100 40GB GPU for each seed, training on three seeds for 18 hours each. Computations were performed on a Slurm-based high-performance computing cluster.

Table 2: SAC Hyperparameters and Settings for RBRL.

Parameter	Default Value	Description
num_envs	4	Number of parallel environments
total_timesteps	500	Total number of environment steps
gamma	0.95	Discount factor γ
tau	1.0	Target smoothing coefficient
batch_size	16	Batch size of sample from the replay memory
buffer_size	4096	The replay memory buffer size
max_episode_steps	32	Episode truncation
learning_starts	256	Timestep to start learning
policy_lr	1×10^{-4}	Learning rate of policy network optimizer
q_lr	1×10^{-4}	Learning rate of Q-network optimizer
actor_updates	4	Number of actor updates per update cycle
critic_updates	4	Number of critic updates per update cycle
target_network_frequency	64	The frequency for the target network update
alpha	0.01	Initial entropy regularization coefficient
autotune	True	Automatic tuning of the entropy coefficient
target_entropy_scale	0.89	Coefficient for scaling the autotune entropy target
dropout	0.05	The dropout rate
num_rules	5	Number of rules for RBRL
llm	"gpt-4o-mini"	LLM for generation
embedder_lm	"m2-bert-80M-8k-retrieval"	The LLM to use for embeddings
embed_dim	768	Dimension of rule embeddings
hidden_dim	16	Hidden dimension of networks
rule_reward_coef	1.0	The reward coefficient for the rules
num_self_attention_layers	1	For the actor and critic
num_cross_attention_layers	1	For the actor and critic

Table 3: Numeric PPO Hyperparameters and Settings.

Parameter	Default Value	Description
total_timesteps	50000	Total timesteps of the experiments
learning_rate	2.5×10^{-4}	Learning rate of the optimizer
num_envs	4	Number of parallel environments
num_steps	512	Steps per policy rollout
anneal_lr	False	no learning rate annealing
gamma	0.95	Discount factor γ
gae_lambda	0.95	Lambda for Generalized Advantage Estimation
num_minibatches	4	Number of mini-batches
update_epochs	64	Number of update epochs
norm_adv	True	Whiten advantages
clip_coef	0.2	Surrogate clipping coefficient
clip_vloss	True	Clipped loss for value function
ent_coef	0.01	Coefficient of entropy term
vf_coef	0.5	Coefficient of value function
max_grad_norm	0.5	Maximum gradient clipping norm
target_kl	None	Target KL divergence threshold
hidden_dim	16	Hidden dimension of networks
num_hidden_layers	2	For policy and critic networks
max_episode_steps	32	Episode truncation

Table 4: LLM PPO Finetuning Hyperparameters and Settings.

Parameter	Default Value	Description
total_timesteps	500	Total number of timesteps
learning_rate	2.5×10^{-4}	Learning rate of optimizer
num_envs	4	Number of parallel game environments
num_steps	32	Steps per policy rollout
anneal_lr	True	Enable learning rate annealing
gamma	0.95	Discount factor γ
gae_lambda	0.95	Lambda for Generalized Advantage Estimation
update_epochs	4	Number of update epochs per cycle
norm_adv	True	Advantages whitening
clip_coef	0.2	Surrogate clipping coefficient
clip_vloss	True	Clipped loss for value function
ent_coef	0.01	Coefficient of entropy term
vf_coef	0.5	Coefficient of value function
kl_coef	0.05	KL divergence with reference model
max_grad_norm	0.5	Maximum gradient clipping norm
target_kl	None	Target KL divergence threshold
dropout	0.0	Dropout rate
llm	"meta-llama/Llama-3.1-8B-Instruct"	Model to fine-tune
train_dtype	"float16"	Training data type
gradient_accumulation_steps	16	Number of gradient accumulation steps
minibatch_size	1	Mini-batch size for fine-tuning
max_chunk_size	256	Maximum length sequence for the back propagation
max_episode_steps	32	Maximum number of steps per episode

C. Additional Survey Results

Figure 7 illustrates the results of a human survey conducted to evaluate the quality of explanations generated by our method compared to alternatives. A total of 21 valid responses were collected for the HeatAlert environment (Figure 7a), and 20 valid responses were gathered for the Uganda environment (Figure 7b). As shown in the figures, our method was favored by the majority of participants across all cases. In the HeatAlert environment, the preference for our approach is evident, although there is a small percentage of tied and “Not Preferred” responses. In contrast, the preference for our method is even more pronounced in the Uganda environment, with a significantly higher number of participants selecting “Ours Preferred.” These results demonstrate the effectiveness of our approach in generating explanations that resonate better with human users, particularly in the Uganda domain.

Figure 8 illustrates the survey outcomes obtained by querying LLMs 20 times for each case in the HeatAlerts (Figure 8a) and Uganda (Figure 8b) environments. To ensure variability, the LLM’s sampling temperature was controlled, enabling randomized responses for each trial. Similar to the human survey results, our method (“Ours Preferred”) is overwhelmingly favored across all cases in both domains. Notably, the consistency of “Ours Preferred” responses highlights the effectiveness of our approach in generating explanations that align well with the LLM’s evaluation criteria, further validating the robustness of our methodology.

Figure 9 illustrates the survey results evaluating hallucination occurrences across two environments (Uganda and HeatAlert) for three explanation types: Chain of Thought (CoT), Rule-Bottleneck Reinforcement Learning (RBRL), and None (indicating no explanation).

In Figure 9a, the results from the human survey indicate that CoT-based explanations had a significant proportion of hallucinations, particularly in the Uganda environment, where it accounted for 42.4% of responses. RBRL explanations showed markedly fewer hallucinations in both domains, highlighting its robustness. A notable percentage of responses for None indicate scenarios where explanations were either absent or irrelevant. In Figure 9b, results from the LLM survey further emphasize the trends observed in the human survey. Hallucination rates for CoT were even higher in the Uganda environment (81.7%), whereas RBRL explanations exhibited almost no hallucinations across both domains. In the HeatAlert environment, the absence of explanations (None) led to the highest percentage of hallucinations, underlining the importance of well-structured, rule-based explanations like RBRL. These results collectively demonstrate that the RBRL framework significantly mitigates hallucinations, providing more accurate and reliable explanations compared to other methods.

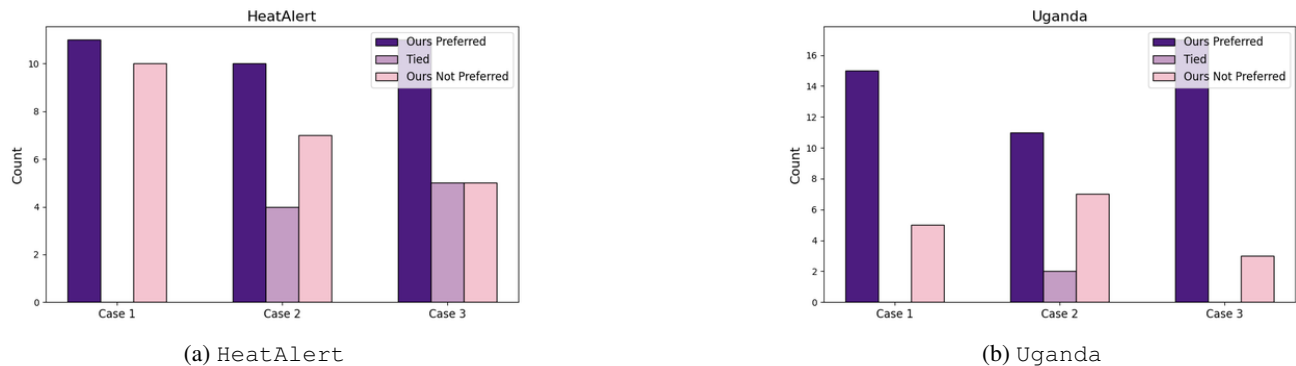


Figure 7: Results from **human** surveys conducted in the HeatAlert (a) and Uganda (b) environments. 21 participants provided feedback for the HeatAlert domain, while 20 valid responses were collected for the Uganda domain. The results indicate that our method (“Ours Preferred”) was favored by a majority of participants, particularly in the Uganda domain, where the preference is more pronounced.

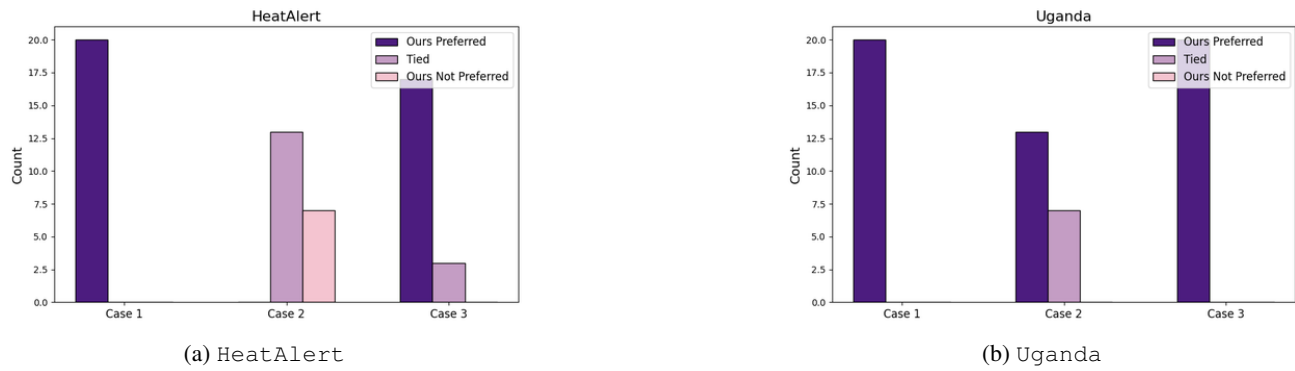
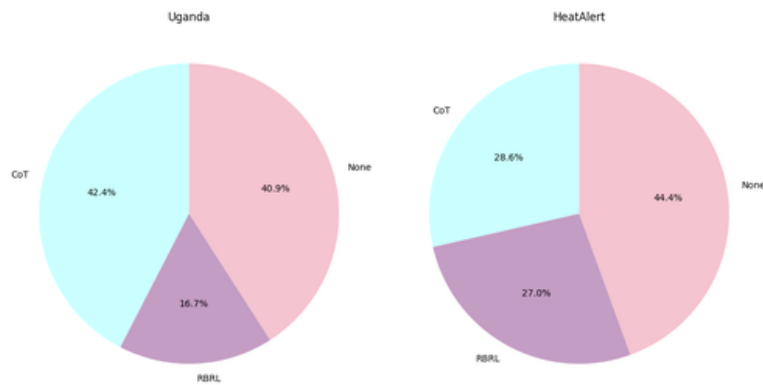
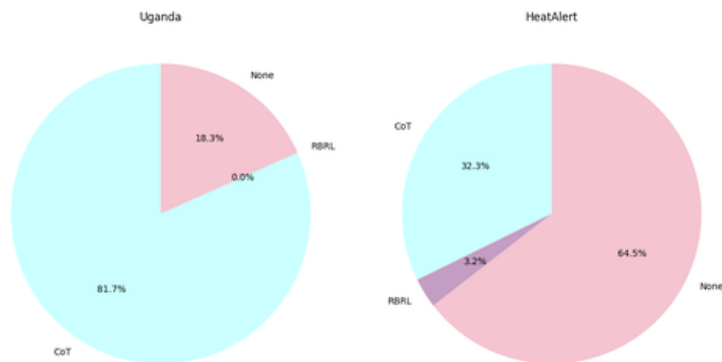


Figure 8: Survey results generated by querying **LLMs** 20 times for each case in the HeatAlert (a) and Uganda (b) environments. By varying the sampling temperature, randomized responses were collected for comparison. The results demonstrate that our method (“Ours Preferred”) consistently outperforms alternatives across all cases, highlighting its robustness and alignment with the evaluation criteria of the LLMs.



(a) Results from the **human** survey, showcasing the proportion of hallucination detected across three categories: CoT, RBRL, and None. In both domains, hallucinations were most frequently identified in None, with RBRL showing significantly fewer instances.



(b) Results from the **LLM**-based survey, where hallucination detection was assessed through multiple iterations of LLM evaluation. CoT exhibited higher hallucination rates in the Uganda domain, while RBRL demonstrated minimal hallucination occurrences in both domains.

Figure 9: Survey results for hallucination detection across the HeatAlert and Uganda environments.

D. Prompt Templates and Rule Examples

D.1. Prompt Format

In this section, we illustrate the prompt format used in our RBRL for generating thoughts, rules, actions, rule scores, and explanations in Figure 10.

Generate Thoughts
First, reason about what elements should be considered when choosing the optimal action . Your response should consist of a single short paragraph that reflects on the consequences, benefits, and drawbacks of each action in the current state.
Generate Rules
Now, suggest {num_rules} rules that could be useful to make an optimal decision in the current state. For each rule, provide the explanation of why it is important to consider it at the given state. Each rule should be in machine-readable JSON Lines format. Each line should follow the following schema: {'background': str, 'rule': str, 'state relevance': str, 'goal relevance': str} - The 'background' should a brief introduction and motivation to the focus of the rule. - The 'rule' should be a statement of the form '[do/select/prioritize] [if/when/condition]' where the condition must be relevant to the current state. - The 'state relevance' should explain why the rule applies to the current problem state. - The rule alone should be sufficient to deduce the optimal action that should be taken in the current problem state. - Start each line with the character '```' - {.
Generate Actions
Below is/are a prioritization rule/rules to make an optimal decision in the current state: {selected rule/rules} Now, choose the optimal action given the current problem state and this/these prioritization rule/rules. Your answer must consist exclusively of one of the following actions: Possible actions:{description about action space} You cannot refuse to respond. Do not provide additional information or context for your answer, only the action.
Generate Rule Scores
To make a decision in the current state, the following rule/rules was/were selected: {rules} You will now be given a question you need to answer with a simple 'yes' or 'no'. q1 = "Is/are the rule/rules **alone** sufficient to understand the optimal action/decision that the system should take in current the problem state?" q2 = "Is the condition in the rule/rules actionable and complete in the current problem state (containing sufficient detail about the current problem state without unnecessary information)?" q3 = "Did the selected rule/rules sufficiently help to understand the previous decision without contradictions?" Answer the following questions with a simple 'yes' or 'no' without additional information or justification. Your response should be a single word.
Generate Explanation
You chose action {outputs['action']} in the current problem state. Explain why you chose the optimal action based on the conversation. Your response should be a short paragraph with 1-3 sentences that explain the reasoning behind your choice.

Figure 10: Prompts template for generating thoughts, rules, actions, rule scores, and explanations.

D.2. Rule Example

In this section, we provide some rules for each domain in Figure 11.

Rule Examples
<p style="text-align: center;">Example 1: Wearable Device Assignment</p> <ul style="list-style-type: none"> - Rule1: "Prioritize reallocating devices from patients who have worn the device for the least amount of time and have stable vital signs." - Rule2: "Select to reallocate devices from patients with less critical vital signs to those with high pulse rates or low SPO2." - Rule3: "Reallocate devices from patients whose mean vital signs are within normal ranges to those whose mean vital signs are abnormal." - Rule4: "Select to reallocate devices from patients with lower standard deviation in vital signs, as they are less likely to experience sudden changes." - Rule5: "When a new patient arrives, reallocate devices from patients who have shown the least improvement over time." <p style="text-align: center;">Example 2: Heat Alert Issuance</p> <ul style="list-style-type: none"> - Rule1: "If the current heat index is above the average heat index of the past week, issue a warning." - Rule2: "If there have been 5 or more warnings in the last 14 days, do not issue a warning unless the heat index exceeds 100 F." - Rule3: "If the heat forecast for the next day exceeds 98 F, issue a warning today." - Rule4: "If today is a weekday and the heat index is above 95 F, do not issue a warning unless the forecasted heat index for the weekend exceeds 100 F." - Rule5: "If the remaining number of warnings is 5 or fewer, prioritize issuing a warning when the heat index exceeds 98 F."

Figure 11: Rule examples for the considered two domains.

E. Survey Example

In this section, we present a survey example from the `Wearable_Device_Assignment` domain. The survey for the `HeatAlert` domain follows the same format and can be easily adapted by substituting the task and corresponding actions. For brevity, we include only one example case from the `Wearable_Device_Assignment` domain.

Task: *You are tasked with optimizing the allocation of limited vital sign monitoring devices among patients. Devices improve vital signs and prevent abnormalities, but their limited availability requires reallocating them from stable patients to higher-risk incoming patients, who must always receive a device. The normal range of vital signs are provided in Figure 12. The goal is to minimize costs associated with abnormal vital signs, where costs are calculated exponentially based on deviations from predefined thresholds. Wearing a device improves abnormal vital signs with a 70% success rate.*

Possible actions: *Choose the id of the device that will be reallocated to the new incoming patient. Your answer should be a single integer i from 0 to 4 (the number of devices) such that:*

- *Always choose a free device if available*
- *If no free device is available, then choose device i whose current patient is at least risk or would benefit less from wearing the device.*

Vital Sign	Normal Range
Heart Rate	60–100 bpm
Respiratory Rate	12–20 breaths/min
SPO2 (Oxygen Saturation)	≥ 95%

Figure 12: Normal range of vital signs.

In the following, you will be presented with three cases. Each case includes two explanations. Please read the text for each case carefully and answer the questions provided.

Case 1: Current state of the decision problem:

Number of devices: 5

Number of free devices: 1

IDs of free devices: 3

Device 0: Device is currently assigned to a patient with the following description:

Timesteps wearing the device: 1

Pulse rate - Last value: 95.22 - Mean: 105.12 - Standard deviation/volatility: 10.56

Respiratory rate - Last value: 20.14 - Mean: 20.54 - Standard deviation/volatility: 0.64

SPO2 - Last value: 98.42 - Mean: 97.89 - Standard deviation/volatility: 0.88

Device 1: Device is currently assigned to a patient with the following description:

Timesteps wearing the device: 1

Pulse rate - Last value: 89.55 - Mean: 81.86 - Standard deviation/volatility: 8.55

Respiratory rate - Last value: 14.85 - Mean: 20.81 - Standard deviation/volatility: 3.40

SPO2 - Last value: 95.31 - Mean: 96.22 - Standard deviation/volatility: 1.38

Device 2: Device is currently assigned to a patient with the following description:

Timesteps wearing the device: 1

Pulse rate - Last value: 106.05 - Mean: 105.09 - Standard deviation/volatility: 2.91

Respiratory rate - Last value: 19.34 - Mean: 20.80 - Standard deviation/volatility: 2.69

SPO2 - Last value: 99.56 - Mean: 99.36 - Standard deviation/volatility: 0.27

Device 3: Device is currently free.

Device 4: Device is currently assigned to a patient with the following description:

Timesteps wearing the device: 1

Pulse rate - Last value: 80.02 - Mean: 79.03 - Standard deviation/volatility: 1.58

Respiratory rate - Last value: 22.71 - Mean: 21.31 - Standard deviation/volatility: 5.45

SPO2 - Last value: 99.61 - Mean: 99.86 - Standard deviation/volatility: 0.14

Explanation A: I chose to reallocate device 4 because the patient currently using it has a stable pulse rate (80.02) and a high SPO2 level (99.61), indicating they are less at risk and may not require continuous monitoring. In contrast, reallocating this device allows for an incoming patient, who likely has more urgent health needs, to receive the device, thereby optimizing the overall allocation of resources to those who require immediate attention.

Explanation B: I chose action 'device': 3 because device 3 is currently free and must be assigned to an incoming patient who requires immediate monitoring to prevent any potential deterioration in their health. This decision aligns with the prioritization rule that emphasizes the importance of providing care to all patients, especially those at risk, ensuring that the incoming patient receives the necessary vital sign monitoring.

Q1. Do Explanation A and Explanation B appear the same or different to you?

Same (Skip Q2 and go to Question Q3)

Different

Q2. Which explanation do you find better?

Explanation A

Explanation B

Q3. Do the explanations contain any hallucinations?

Both

Only Explanation A

Only Explanation B

None